MAGNETIC PROPERTIES OF SOME NIOBIUM (IV) AND TANTALUM (IV) COMPLEXES OF DISTORTED OCTAHEDRAL SYMMETRY

by

Othman Nor

This Thesis is Submitted in Partial Fulfillment of the Requirements for the Degree of Master of Science at the Department of Chemistry, University of Ottawa.

March, 1966

A.D. Westland
Associate Professor
Research Supervisor.

Othman Nor
Candidate.

PREFACE

Since 1932 when Van Vleck published his work "Electric and Magnetic Susceptibilities," various treatments of paramagnetism in the complexes of the transition metals have been given, each attempt a refinement on the preceding one by taking into account an additional factor, or factors, hitherto neglected. In 1961, Figgis worked out the susceptibility of the $^2T_{2g}$ ground term, arising from d^1 and d^5, when further perturbed by an axial-field component.

This theory has been used, with considerable success, to analyse the magnetic data of the first row transition metals, but no attempt has been made to treat the second and third row elements in this way*. It is, therefore, of interest to investigate the magnetic properties of Nb(IV) and Ta(IV) in the light of this theory.

McCarley and Torp and McCarley and Boatman obtained results for $MX_4(pyridine)_2$ (M = Nb,Ta; X = Cl,Br,I) which fitted the Curie-Weiss relationship, giving effective moments well below the spin-only value. Theoretical considerations indicate that for the tetragonal d^1 configuration the axial field splitting is required to be several times larger than the spin-orbit coupling for this to be the case. As the

---

* In the course of this work the magnetic properties of $NbX_4(acetonitrile)_2$ (X = Cl,Br,I) were reported (63)

spin-orbit coupling constant for the elements of the second and third row are rather large, this is rather surprising. Therefore, it is considered desirable to reinvestigate some of these complexes along with the complexes of 2,2'-bipyridyl and N,N,N',N'-tetramethylchtylenediamine.

Acknowledgement

To Dr. A.B. Scotland, whose enthusiasm in the progress of the investigation has been a constant source of inspiration throughout the work, and whose availability for discussions and consultations during the entire course of the project and the preparation of this thesis extended to well beyond regular hours, the author wishes to express his deepest and sincere gratitude. He is also indebted to Miss M. Wilks and Miss D. Ellis for their assistance in the magnetic measurements.

Finally, financial assistance from the International Nickel Co. of Canada Ltd. in the form of a Graduate Research Fellowship, from the Canadian Colombo Plan Technical Aid Programme, and from the Ontario Research Foundation is gratefully acknowledged.

TABLE OF CONTENTS

LIST OF TABLES

LIST OF FIGURES

ABSTRACT

The treatment of paramagnetism using the approach of the crystal field theory is discussed, with special emphasis on the tetragonally distorted octahedral field. For the limiting cases when $\Delta \gg \lambda$ for positive and negative Δ, expressions for the susceptibility are derived.

Complexes of NbX_4 and TaX_4 (X = Cl, Br) with pyridine, bipyridyl and tetramethylethylenediamine were prepared and their magnetic susceptibilities studied over a temperature range 90 - 300°K. The data for all twelve complexes indicate that the Curie-Weiss law is not obeyed; their effective moments exhibit small temperature dependence and the values at room temperature are well below the spin-only value for a single unpaired electron.

Empirical fittings of μ_{eff} against $kT/|\lambda|$ curves from Figgis (34) show that

(a) the sign of Δ is reversed from that deduced on the basis of the crystal field model,

(b) the axial field splittings are greater for the chlorides, and

(c) Δ decreases in the order pyridine > bipyridyl > amine, for a given halide.

The reversal in the sign of Δ is attributed to the π-donating effect from the halogens. (b) is accounted for

by the order of the halide ions in the spectrochemical series. The lower Δ values for 4meen complexes are explained by the higher basicity of the ligand compared to pyridine and bipyridyl. Pyridine complexes have larger Δ values than the corresponding bipyridyl complexes probably because of the slightly better π-accepting capacity of pyridine.

GLOSSARY OF SYMBOLS

χ	Magnetic susceptibility
χ'_M	Molar susceptibility corrected for diamagnetism
χ_g	Gram susceptibility
μ	Magnetic moment
μ_{eff}	Effective magnetic moment
β	Bohr magneton
g	Spectroscopic splitting factor
ξ	Single-electron spin-orbit coupling constant
λ	Many-electron spin-orbit coupling constant
λ'	Spin-orbit coupling constant for complex ion
Δ	Tetragonal field splitting parameter
$v = \Delta/\lambda'$.	
k	Electron delocalization factor

INTRODUCTION

The phenomenon of paramagnetism has been of interest to chemists for a very long time, and its application in the structural determinations of complexes of the transition metals, especially those of the first row, is well known. The more elementary aspect of this phenomenon, and of magnetochemistry in general, has been adequately dealt with in standard texts and review articles (1-4). The present work is a study of the magnetic properties of d^1 complexes of a second and a third row transition metal in more detail. The treatment of paramagnetism by the method of Pauling (1,2) has now been replaced by the use of the crystal field theory, and it is the latter approach that will be followed.

A. Formula for Magnetic Susceptibility

Paramagnetism arises from the spin and orbital angular momenta of the electrons in a system. A paramagnetic atom or molecule may be regarded as a micro magnetic dipole with moment $\vec{\mu} = (\vec{L} + 2\vec{S})\beta$, where $\vec{L}$ and $\vec{S}$ are the total orbital and spin angular momentum respectively and β the Bohr magneton. In the presence of a magnetic field these micro magnetic dipoles experience the opposing effects of the field and temperature; the former tends to align all the dipoles in the same direction as that of the field while

thermal agitation tends to randomise their direction. There is thus a thermal distribution of aligned dipoles in the various energy levels of the system.

For any given stationary state of energy $\epsilon_{n,m}$, the magnetic moment of each atom or molecule ($\mu_{n,m}$) in the direction of the field H is

$$\mu_{n,m} = -\frac{\partial \epsilon_{n,m}}{\partial H} = -(\epsilon^{(1)}_{n,m} + 2H\epsilon^{(2)}_{n,m} + \ldots)$$

where $\epsilon^{(i)}_{n,m}$ ($i = 1,2,3 \ldots$) is the Zeeman perturbation energy of the ith order.

The total magnetic moment per mole (P) is then the statistical mean over all the stationary states weighted according to the Boltzmann factor $e^{-\epsilon_{n,m}/kT}$.

$$P = N\frac{\sum_{n,m} \mu_{n,m}\, e^{-\epsilon_{n,m}/kT}}{\sum_{n,m} e^{-\epsilon_{n,m}/kT}} \qquad [1]$$

N = Avogadro's number.

The susceptibility ($\chi_i = P_i/H_i$) in a given direction ($i = x,y,z$) is then given by

$$\chi_i = N\frac{\sum_{n,m}\left[(\epsilon^{(1)}_{n,m})^2/kT - 2\epsilon^{(2)}_{n,m}\right] e^{-\epsilon^{0}_{n,m}/kT}}{\sum_{n,m} e^{-\epsilon^{0}_{n,m}/kT}} \qquad [2]$$

if the following restrictions are made:-

(a) The susceptibility is independent of H, that is saturation effects are neglected.

(b) There is no intrinsic magnetization.

(c) Only terms linear in H are retained in the simplification of [1].

(d) $kT \gg \mu_{n,m}^{(1)}$.

The derivation of this formula is due to Van Vleck (5,6).

From the derivation of formula [2] it is apparent that magnetic susceptibility gives us information concerning the average population of the various stationary states, and, therefore, the magnitude of the susceptibility (or moment) is dependent upon the multiplicity and the separation of the levels of the ground state and the few next excited states of the system. When the separation of the levels in the ground state is small compared to kT and the difference in energy between the ground state and the first excited level is large compared to kT it has been shown by Van Vleck that, neglecting diamagnetic contribution, χ_i is given by

$$\chi_i = N\left[\sum_{n,m} (\mu_{0,m}^{(1)})^2 / J_m kT - 2\sum_{n,m} \mu_{0,m}^{(2)} / J_m\right] \qquad [3]$$

where $\mu_{0,m}^{(1)} = \langle \psi_{0,m} | \mu_i | \psi_{0,m} \rangle$

$$\mu_{0,m}^{(2)} = \sum_{n,m} \frac{|\langle \psi_{0,m} | \mu_i | \psi_{n,m} \rangle|^2}{|E_0 - E_m|}$$

$\mu_i = \beta(\hat{l} + 2\hat{s})$, $\beta = eh/4\pi mc$

J_m = multiplicity of the ground state

The sign $\hat{}$ designates an operator of vector character.

The second term in [3] is the Van Vleck "high frequency" term, or the temperature-independent paramagnetism (TIP), and it is simply the second order Zeeman effect arising from the matrix elements of μ_1 between the ground and higher levels.

Equations [2] and [3] form the theoretical basis for the calculation or estimation of magnetic susceptibility of a system. It is clear that a knowledge of the energy levels of the system is necessary for the application of the appropriate formula (either equation [2] or [3]). The crystal field theory as developed by Bethe (7) and Schlapp and Penney (8), with its subsequent modifications, has provided an approach to this end, and a discussion of the theory and its application to transition metal complexes follows.

B. Crystal Field Theory

Essentially the foundation of the crystal field theory lies in the assumption that an inorganic complex may be regarded as an ionic molecule consisting of a central metal ion surrounded by atoms or molecules, called ligands, such that there is only electrostatic interaction between the ligands and the electrons of the central ion. The electrons of the central ion, therefore, no longer experience the field of spherical symmetry from the nucleus alone, but in addition they are also subjected to an electric field

from the ligands, this field being of the same symmetry as the arrangement of the ligands about the central ion. Hence, in the absence of any other external field, the Hamiltonian for the electrons of the metal ion is given by

$$\mathcal{H} = -\frac{\hbar^2}{2m}\sum_i \nabla_i - \sum_i \frac{Ze^2}{r_i} + \sum_{i\neq j}\frac{e^2}{r_{ij}} + \sum_i \xi_i(r)\hat{l}_i\cdot\hat{s}_i + V$$

where $\hbar = h/2\pi$, h = Planck's constant. All the other symbols carry the usual significance.

The first two terms are the coulomb interaction of the electrons with the nucleus, the third is the electron-electron repulsion term (i.e. coulombic interaction of the electrons with each other) and the fourth is the magnetic interaction between the electron spins (s) and their orbital motion (l). These four terms constitute the Hamiltonian for the free ion. The last term, V, is the perturbation produced by the electric field of the surrounding ligands.

(a) Octahedral Field Perturbation

The potential V can be expanded in normalized spherical harmonics, $Y_l^m(\vartheta_i, \varphi_i)$.

$$V = \sum_i \sum_l \sum_m Y_l^m(\vartheta_i, \varphi_i) E_{nl}(r_i) \qquad [4]$$

The expansion of [4] can be greatly simplified on general symmetry grounds. The term having $l = 0$ is spherically

symmetric and it is merely an additive constant since it only gives rise to a uniform shift of all levels with the same number of electrons. All terms with l = odd or l > 4 give zero matrix elements when the effect of V on d-orbitals is considered, the former because d-orbitals are of even parity and the latter because the product $\psi_a^* \psi_b$ of two different d-electron wave-functions does not contain spherical harmonics with l > 4. Finally V must transform as the totally symmetric representation in the symmetry group of the molecule. Thus the octahedral field acting on d-orbitals is given by

$$V = V_0 + Y_4^0 + \sqrt{5/14}(Y_4^4 + Y_4^{-4}),$$

if the system is quantized along the four-fold z-axis, or using Cartesian coordinates,

$$V = V_0 + (x^4 + y^4 + z^4 - \tfrac{3}{5}r^4). \qquad [5]$$

V_0 is the term with l = 0.

Perturbation theory necessitates the treatment of each term in the Hamiltonian in the order of decreasing magnitude. Three cases have been distinguished with regards to the magnitude of V relative to the other terms in $\mathcal{H}$.

(a) V is large compared to electron-electron repulsion but small compared to coulomb interaction of the electrons with the nucleus.

(b) V is intermediate between the coulomb interactions

and the spin-orbit interactions.

(c) Γ is small compared to the spin-orbit interactions.

Since complexes of the second and third row transition metals are mainly of case (a), i.e. strong-field or spin-paired (9), a description, in brief, of the perturbation treatment for (a) is given below. For case (b), which is typical of the first row transition metal complexes, the results will merely be summarized. A more complete treatment by the perturbation method of the crystal field effects on the electrons of the central ion for the three cases enumerated above has been given by Ballhausen (6), Bleaney and Stevens (10) and Howard (11), among others.

The five d-orbitals span the irreducible representations e_g and t_{2g} of the octahedral group O_h. Hence when perturbed by a crystal field of octahedral symmetry the five-fold orbital degeneracy is lifted to a triply degenerate t_{2g} set (d_{xy}, d_{xz}, d_{yz}) and a doubly degenerate e_g set ($d_{x^2-y^2}$, d_{z^2}), the t_{2g} set lying lower. The difference in energy between the two sets (the crystal field splitting) is taken as 10Dq by convention (8), so that the t_{2g} set lies at -4Dq and the e_g at 6Dq.

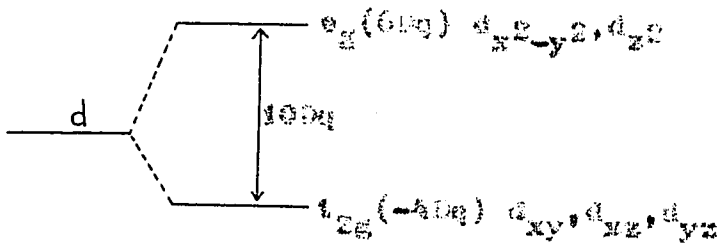

The electrons in the complex go into the t_{2g} set first until six electrons have been accomodated (subject to the exclusion principle), and only then do they go into the e_g set. The ground state is to be found by the application of a modified Hund's rule: viz. that the electrons are arranged to give maximum total spin. For example in the d^2 configuration the ground state is a triplet arising from $(t_{2g})^2$ — viz. $^3T_{1g}$. The other components from $(t_{2g})^2$ are $^1A_{1g}$, ^1E_g and $^1T_{2g}$. The terms are deduced by consideration of the direct product representation, $t_{2g} \times t_{2g}$, in O_h. The energy of a term is obtained by summing up the energies of the electrons, $\Sigma(t_{2g})$ being $-4Dq$ and $\Sigma(e_g) = 6Dq$. To this is then added the coulomb interaction energy among the electrons as given by the term $\frac{1}{2}\sum_{i \neq j} e^2/r_{ij}$ in the Hamiltonian. It is this term which separates the various components within the $(t_{2g})^n(e_g)^m$ configuration.

In the weak-field treatment (i.e. case (b)) the perturbation of V is not upon the d^n configuration but rather upon the various spectroscopic terms produced by the electronic repulsion term in the Hamiltonian. The splittings of these terms by the octahedral field V are as below.

$$S \quad — \quad A_1$$

$$P \quad — \quad T_1$$

$$D \quad — \quad E + T_2$$

$$F \quad — \quad A_2 + T_1 + T_2$$

The perturbation by V on d^2, in the weak-field treatment, can be depicted as in figure (1). To emphasise the continuity in going from the weak-field to the strong-field a rough correlation for the triplet components arising from the d^2 configuration is indicated.

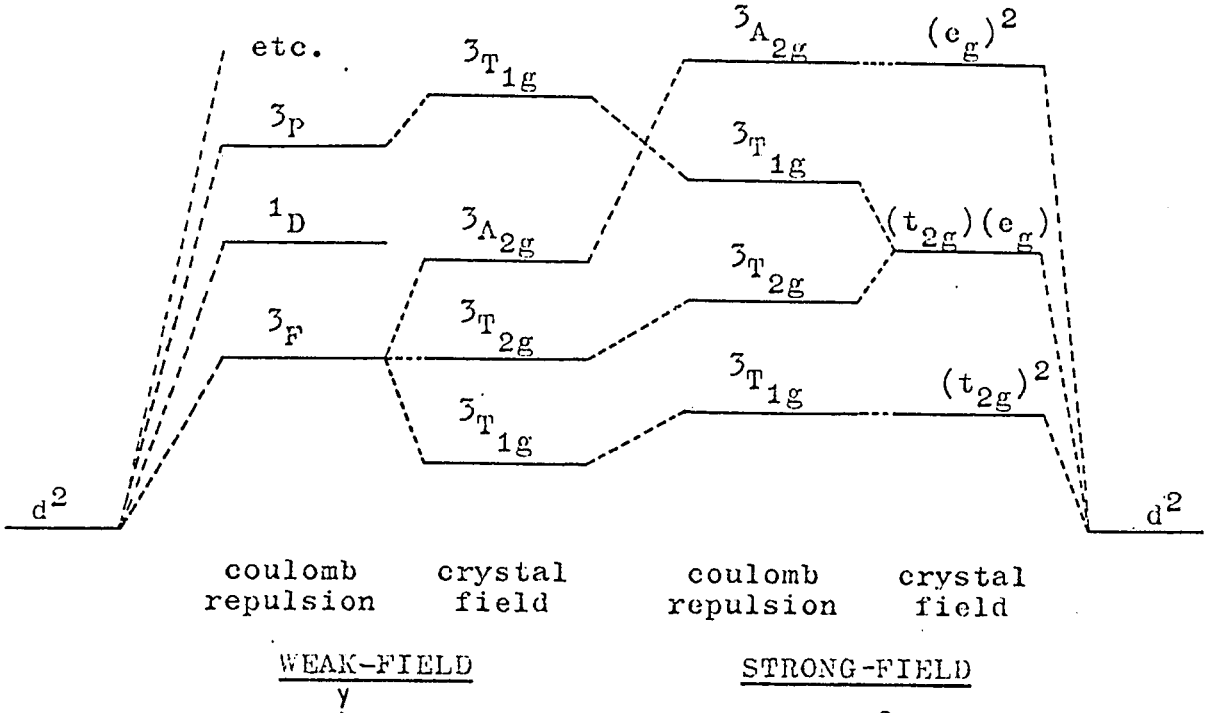

Figure 1. Crystal field perturbation on d^2

(b) Spin-Orbit Interactions

The spin-orbit interactions perturbation for a field of octahedral symmetry takes the form

$$\xi_d \sum_i \hat{t}_i . \hat{s}_i$$

where $\hat{t}_x$, $\hat{t}_y$ and $\hat{t}_z$ transform like T_1. This is because $\hat{s}_x$,

$\hat{s}_y$ and $\hat{s}_z$ transform like T_1 in O_h and, as mentioned earlier, $\hat{t}_i.\hat{s}_i$ must transform like A_1, the total symmetric representation of the point group. For a d-electron (pure d-orbital) $\hat{t}_x$, $\hat{t}_y$ and $\hat{t}_z$ are identical with $\hat{l}_x$, $\hat{l}_y$ and $\hat{l}_z$ respectively. ξ_d is the spin-orbit coupling constant for a single d-electron. If the actual orbitals do not depart too far from the pure d-orbitals ξ_d may be expected to approximate that for the free ion , but Owen (12) has observed that ξ_d for complex ions are smaller than the free-ion values.

For a many-electron system the spin-orbit coupling constant is λ, and for the ground state λ is related to ξ_d by the following.

$$\lambda = \pm \xi_d/2S$$

where S = total spin angular momentum in units of $h/2\pi$. The positive sign is for a shell less than half full, and the negative sign for a shell more than half full. The shell may be either the five-fold degenerate d-shell or the three-fold degenerate t_{2g} set.

The matrix element of $\lambda\hat{L}.\hat{S}$ (or $\xi_d\hat{l}.\hat{s}$) can be easily worked out by using the expansion

$$\lambda\hat{L}.\hat{S} = \lambda(\hat{L}_z\hat{S}_z + \tfrac{1}{2}\hat{L}_+\hat{S}_- + \tfrac{1}{2}\hat{L}_-\hat{S}_+)$$

where $\hat{L}_\pm = \hat{L}_x \pm i\hat{L}_y$ and $\hat{S}_\pm = \hat{S}_x \pm i\hat{S}_y$

Application of the spin-orbit perturbation produces further splitting of those terms which are orbitally degenerate. For

the first row transition metals the spin-orbit coupling is small (ξ_d = 50 - 800 cm^{-1}) but for the second and third row transition metals it is considerably larger (ξ_d = 1000 - 10,000 cm^{-1}). It is not possible, therefore, to treat the spin-orbit coupling as a small perturbation on the electrostatic repulsions within the t_{2g} set. Thus the magnetic properties of strong-field and weak-field complexes of the transition series as worked out by Kotani (13) and Figgis (14) respectively, apply best to the complexes of the first row metals. R. Moffitt et al.(15) and Kamimura and co-workers (16), by considering large λ, have derived expressions more applicable to the transition metals of the second and third row.

(c) Distortion of the Octahedron

By using the strong-field scheme the ground term for the $(t_{2g})^1$ and $(t_{2g})^5$ configuration is $^2T_{2g}$. It is noticed that the ground term has three-fold orbital degeneracy. According to the theorem of Jahn and Teller (17) some distortion of the complex may occur in cases where the ground term has orbital degeneracy. So even when all of the six ligands are alike the crystal field cannot be expected to be of perfect octahedral symmetry. This is not to suggest, of course, that the Jahn-Teller distortion is the only factor tending to distort the octahedral field, as there are others. Such deviations from octahedral symmetry are often

treated as perturbations on the higher symmetry.

From the chemical point of view it seems adequate to consider only trigonal or tetragonal distortion of the octahedron, i.e. to apply a field of axial symmetry on the central ion, in order to account for most of the features of its magnetic behaviour. Furthermore the present work is done on powdered samples only, and treatment of lower symmetry is, therefore, superfluous. Howard (11) and Schlapp and Penney (8) have applied a field of orthorhombic symmetry, considered as a perturbation on the axial field component, in their treatment.

The crystal field potential, V, under axial symmetry has been given by Figgis (18): using Cartesian coordinates,

$$V = V_0 + D(x^4 + y^4 + z^4 - 3r^4/5) + C(x^2 - r^2/3). \quad [6]$$

The axial component of the field is the term in C.

The qualitative effect of the axial component on the terms of the $(t_{2g})^n$ configuration can be deduced by using the method of "descent in symmetry" (19). Thus the orbital triplet is split into a doublet and a singlet, E into two singlets, and A remains unaffected. Typical splittings of the $^2T_{2g}$ term, the ground term for $(t_{2g})^1$ and $(t_{2g})^5$ are shown in figure 2.

The effects of the various perturbations on the ground state of the central ion under an axial crystal field are seen from figure (2) in which the splittings for the d^1 case are shown. As the strengths of the axial distortion and the

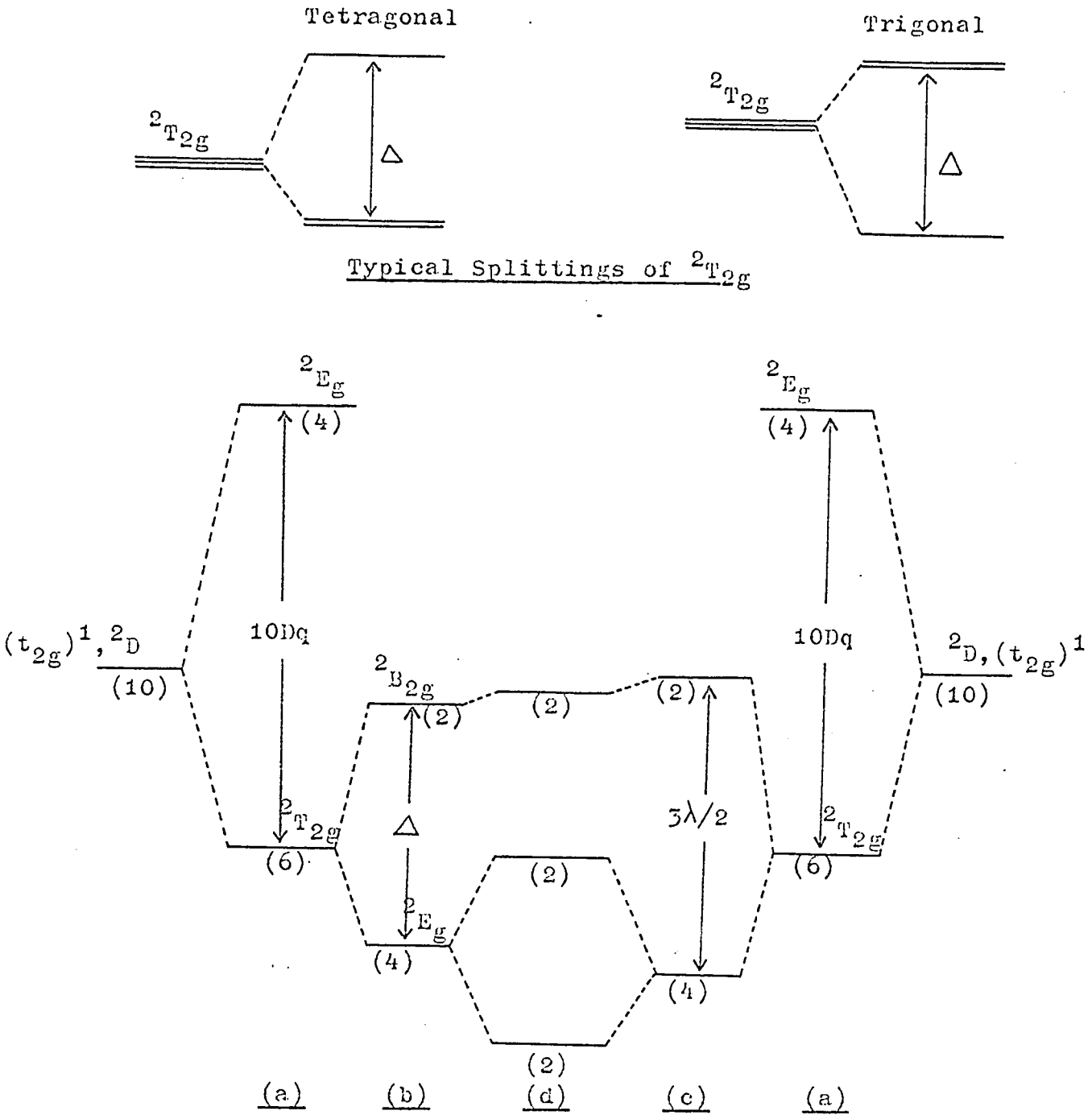

Figure 2. d^1 under Axial Field and Spin-orbit Coupling. (a) Octahedral field, (b) Axial component, (c) Spin-orbit coupling, and (d) Axial field and spin-orbit coupling. Numbers in brackets denote total multiplicity.

spin-orbit perturbations relative to each other vary, both the cases when the spin-orbit interaction is greater than the axial component and the reverse, are shown in the figure.

(d) Magnetic Field Perturbation

The application of a magnetic field H on the system removes the remaining Kramers degeneracies of the levels in figure (2). This perturbation by the magnetic field is given by

$$\mathcal{H}_H = \beta H(\hat{L} + 2\hat{S}).$$

When the system is of cubic symmetry the magnetic susceptibility is the same in any direction, but when it is of a lower symmetry the susceptibility in each direction is in general different. In the first approximation it is possible to assume that the magnetic axes of the molecule coincide with the symmetry axes (20). Hence the magnetic moment operator can be defined for the three orthogonal directions x, y and z:

$$\mu_x = (\hat{L}_x + 2\hat{S}_x)$$
$$\mu_y = (\hat{L}_y + 2\hat{S}_y)$$
$$\mu_z = (\hat{L}_z + 2\hat{S}_z).$$

The separation within a given multiplet, on the application of H, is expressed in the form

$$h\nu = g\beta H$$

where g is the spectroscopic splitting factor, and its values for the x-, y- and z-directions are g_x, g_y and g_z respectively.

The average value $\bar{g}$, is given by

$$\bar{g} = [(g_x^2 + g_y^2 + g_z^2)/3]^{\frac{1}{2}} .$$

The susceptibility χ, obtained from formula [2] or [3], would also be dependent on the direction of H; the average susceptibility, $\bar{\chi}$, is found by the relation

$$\bar{\chi} = \frac{1}{3}(\chi_x + \chi_y + \chi_z).$$

For a given system under axial symmetry, the x- and the y-directions are equivalent. Thus defining the x- and the y-directions as $\perp$ (perpendicular) and the z-direction as $\parallel$ (parallel), $\bar{g}$ and $\bar{\chi}$ become

$$\bar{g} = [\tfrac{1}{3}(g_{\parallel}^2 + 2g_{\perp}^2)]^{\frac{1}{2}}$$

$$\bar{\chi} = \tfrac{1}{3}(\chi_{\parallel} + 2\chi_{\perp}).$$

There are now various lines of experimental evidence indicating that there is more than just electrostatic interaction (an assumption of the crystal field theory) between the ligands and the electrons of the central ion in most cases (21-23). In particular, the analysis of the hyperfine structure of the paramagnetic resonance spectrum of $IrCl_6^{=}$ ion by Griffiths, Owen and Ward (22) has indicated that there is delocalization of the electrons of the central ion over the iridium-chlorine framework. Such a delocalization can be taken into account by the introduction of a factor k (the

orbital reduction factor) into the magnetic moment operator (24), so that

$$\mu = (k\hat{L} + 2\hat{S}),$$

k has a value $\leqslant 1$, and can be interpreted in the sense that for the fraction 1-k of their time the electrons of the central ion do not contribute to the orbital angular momentum of the ion.

(c) Ligand Field Theory

The inadequacy of the crystal field approach in the description of the interactions between the central ion and its ligands has long been recognised (25,26). A more useful approach is given by the ligand field theory which incorporates the more realistic bonding scheme of the molecular-orbital theory of Mulliken (27) into the essential features of the crystal field theory. Hence in this approach the structural unit for the wave-function is the whole complex instead of just the single central atom.

The theory as applied to the transition metal complex has been discussed in various degrees of sophistication (28-31); only the main points are given here. The orbitals of the complex are of the form

$$\Psi = \alpha\Psi(\Gamma) + \beta\sum_j a_j\psi_j$$

where $\Psi(\Gamma)$ is a wave-function of the central atom, and $\sum_j a_j\psi_j$ is a linear combination of the ligand wave-functions. By applying the general group theoretical rule that the

symmetry of the orbitals on metal and ligand must match for combinations to be possible, the important results of this theory can be derived without having to go through the mathematical arguments.

In the O_h symmetry the s-orbitals of the central atom transform under a_{1g}, the p-orbitals under t_{1u} and the d-orbitals under e_g and t_{2g}. The ligand σ-orbitals span the representations a_{1g}, e_g and t_{1u}, and the π-orbitals span the representations t_{1g}, t_{1u}, t_{2g} and t_{2u}. Using these, the molecular-orbital energy-level scheme can be constructed as in figure (3).

One important result, as indicated in the diagram, is that the crystal field splitting 10Dq is the difference in the energies of $e_g(\sigma^*)$ and $t_{2g}(\pi^*)$, and, therefore, the nature of the metal-ligand bond should affect the crystal field splitting, and hence the electronic properties of the complex. Also the delocalization factor k can now be readily understood.

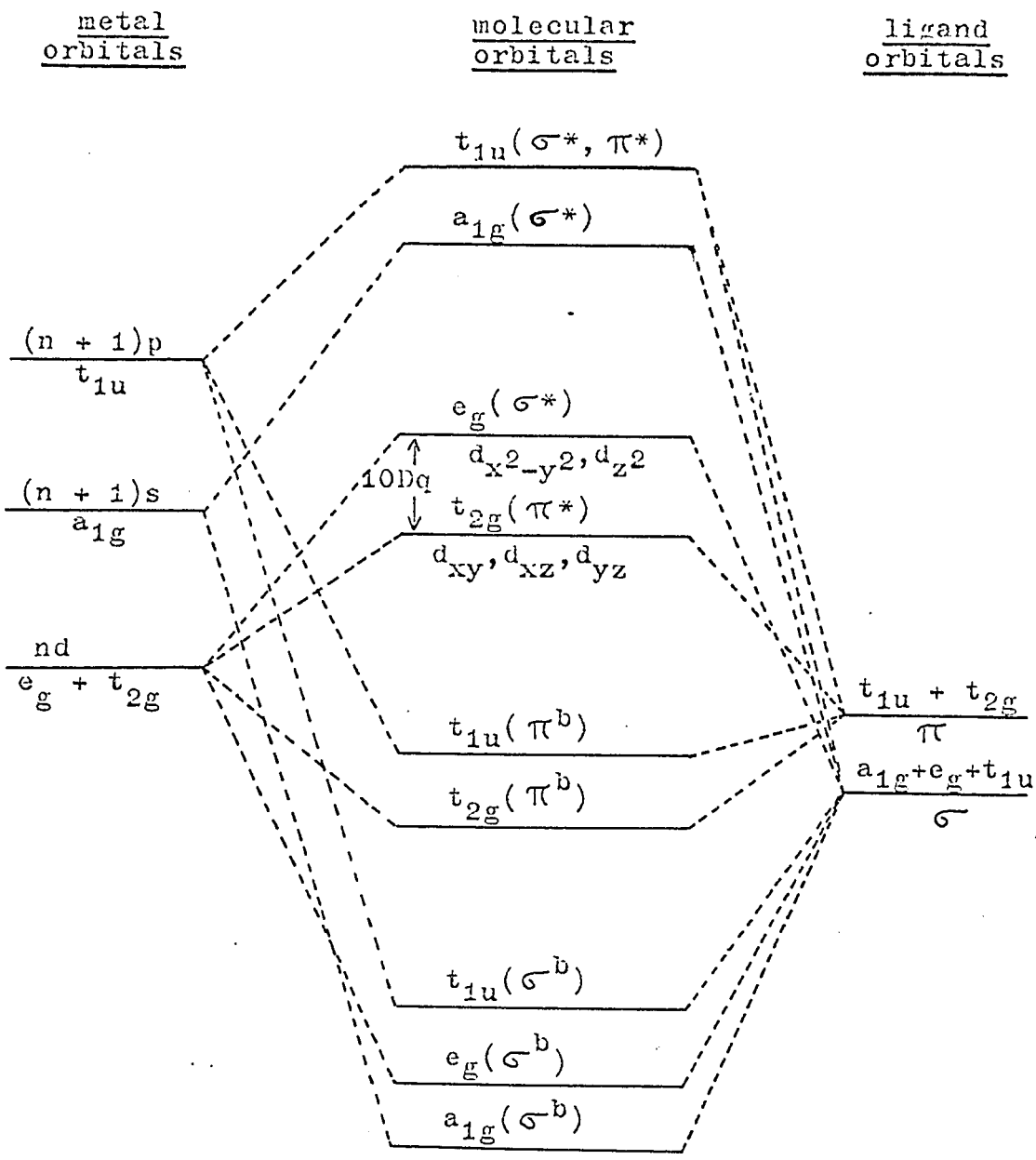

Figure 3. Molecular-orbital Energy-level Scheme for an Octahedral Complex. (diagramatic)

C. Magnetic Properties of Hexa-coordinated d^1 Complexes having Axial Symmetry

Although the present work deals with tetragonally distorted octahedral complexes (more will be said about the symmetry of the ligand field in the complexes studied, in a later section), the account of the theory given below for the D_{4h} point group also applies to the trigonal case, because the results for the two cases differ only in the sign of Δ, the axial field splitting parameter (3E).

(a) Theoretical

In figure (4) a schematic representation of the effects produced by the various perturbations on the d^1 configuration is shown; the final result being three Kramer's doublets from the lower $^2T_{2g}$ term and two from the ^2E_g term 10Dq above. For strong-field complexes, $10Dq \gg kT$, and the effect in magnetic phenomena of these higher terms may often be neglected. It is only taken into account when the spin-orbit coupling parameter, λ, is large with respect to kT; then the mixing of the wave-functions of these higher levels into those of the ground levels, via the spin-orbit interactions operator, is incorporated in the ground state functions.

The appropriate wave-functions can be derived from symmetry considerations*. Thus from the character table for

---

* Exact wave-functions are not required as the magnetic properties of a substance do not depend upon the radial part of the function.

the point group D_{4h} (19) and the table of transformation properties of the d-orbitals in D_{4h} (Appendix 1) it is readily seen that the functions of the various terms are as follows:

Terms	Wave-functions		
$(\Gamma_3)b_{1g}$	$\sqrt{\frac{1}{2}}(d_2 + d_{-2})$	$\equiv$	$\|d\rangle$
$(\Gamma_1)a_{1g}$	d_0	$\equiv$	$\|o\rangle$
$(\Gamma_4)b_{2g}$	$\sqrt{\frac{1}{2}}(d_2 - d_{-2})$	$\equiv$	$\|c\rangle$
$(\Gamma_5)e_g$	d_1	$\equiv$	$\|a\rangle$
	d_{-1}	$\equiv$	$\|b\rangle$

Inclusion of the spin-functions, $[\alpha]$ $(s = \frac{1}{2})$ and $[\beta]$ $(s = -\frac{1}{2})$, is next considered by taking the direct products of Γ_3, Γ_1, Γ_4 and Γ_5 with Γ_6, the representation of the spin-functions in D_4' (33).

$$\Gamma_3 \times \Gamma_6 = \Gamma_7$$
$$\Gamma_1 \times \Gamma_6 = \Gamma_6$$
$$\Gamma_4 \times \Gamma_6 = \Gamma_7$$
$$\Gamma_5 \times \Gamma_6 = \Gamma_6 + \Gamma_7$$

The wave-functions are then found by taking the correct combinations of the orbital parts, from among $|d\rangle$, $|o\rangle$, $|c\rangle$, $|a\rangle$ and $|b\rangle$, with $[\alpha]$ and $[\beta]$ so as to give functions which span the required representations. Figures (4) and (5) list the correct functions so obtained.

Figure (4) gives a schematic representation when Δ is larger than λ. When $\lambda \gg \Delta$ the effects of the combined perturbations on the $^2T_{2g}$ term are shown in figure (5).

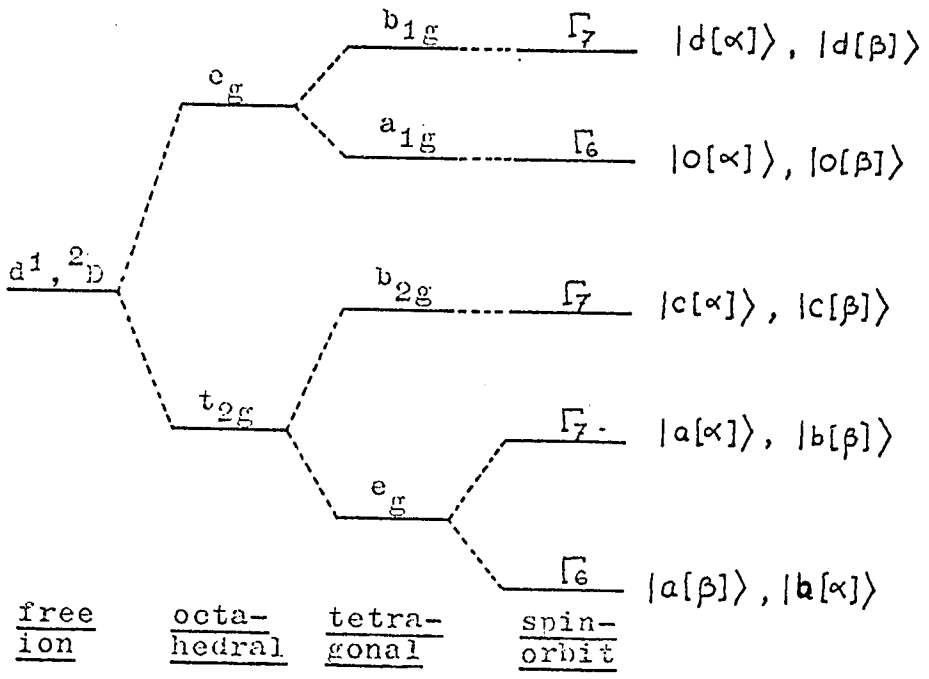

Figure 4. Wave-functions when Δ is larger than λ, -ve Δ.

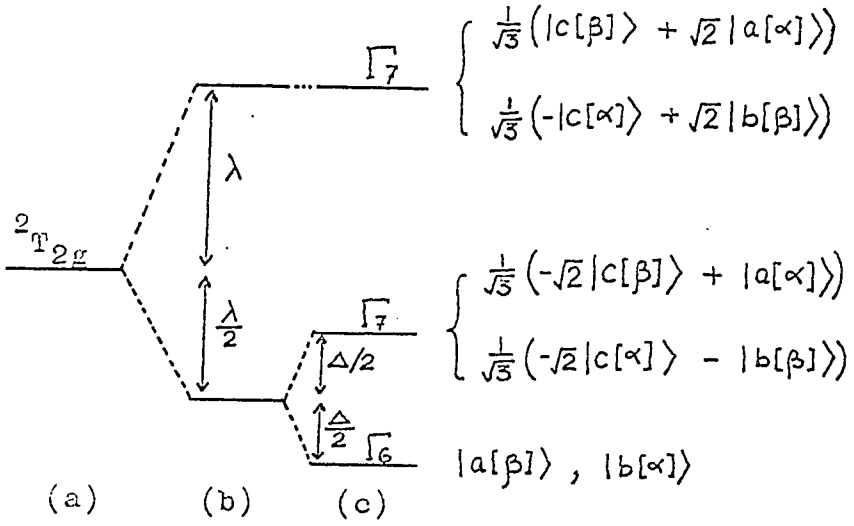

Figure 5. Splitting of $^2T_{2g}$ when $\lambda \gg \Delta$.
(a) Octahedral
(b) Spin-orbit
(c) Tetragonal

Figgis (34) has shown that when the ratio Δ/λ is small (< 1) the effect of the axial field on the effective magnetic moment is small. A treatment of this case, therefore, would lead to a result not very different from that obtained by Kotani (13) or Moffitt et al.(15), depending on the magnitude of λ with respect to KT. In both treatments a perfect octahedral symmetry was assumed.

Whilst a treatment of the general case would be merely a repetition of Figgis's paper (34), on the other hand, consideration of the limiting cases is instructive in so far as they are illustrative of the method used to derive the effective moment. Two limiting cases may be considered: (i) when $\Delta \gg \lambda$ for negative Δ, and (ii) when $\Delta \gg \lambda$ for positive Δ. The sign of Δ, here, is following that used by Kamimura (16) and Figgis (34), viz. that Δ is positive when a singlet is lowest for the tetragonal case.

(i) $\Delta \gg \lambda$, -ve Δ

From figure (4) it can be seen that the magnetic susceptibility arises from the Γ_6 and $\Gamma_7(e_g)$ levels, the $\Gamma_7(b_{2g})$ level lying high above these. The only non-zero elements for the perturbation

$$\mathcal{H}'_{\parallel} = \lambda \hat{l}.\hat{s} + \beta H_z(\hat{l}_z + 2\hat{s}_z)$$

are the diagonal ones (24):-

$$\langle a[\alpha]|\mathcal{H}'_{\parallel}|a[\alpha]\rangle = \frac{\lambda}{2} + 2\beta H_z$$
$$\langle b[\beta]|\mathcal{H}'_{\parallel}|b[\beta]\rangle = \frac{\lambda}{2} - 2\beta H_z$$
$$\langle b[\alpha]|\mathcal{H}'_{\parallel}|b[\alpha]\rangle = \langle a[\beta]|\mathcal{H}'_{\parallel}|a[\beta]\rangle = -\frac{\lambda}{2}$$

Substituting the above results into equation [2], and simplifying, we obtain

$$\chi_{\parallel} = \frac{N\beta^2}{3kT} \cdot \frac{12}{e^x + 1},$$

where $x = \lambda/kT$.

For the perturbation

$$\mathcal{H}'_{\perp} = \lambda \hat{l}.\hat{s} + \beta H_x(\hat{l}_x + 2\hat{s}_x)$$

the eigenvalues are the solutions to the following secular equation:

$$\begin{vmatrix} \Gamma_6^a & \Gamma_7^a & \Gamma_6^b & \Gamma_7^b \\ -\frac{\lambda}{2} - E & \beta H_x & 0 & 0 \\ \beta H_x & +\frac{\lambda}{2} - E & 0 & 0 \\ 0 & 0 & -\frac{\lambda}{2} - E & \beta H_x \\ 0 & 0 & \beta H_x & +\frac{\lambda}{2} - E \end{vmatrix} = 0,$$

that is

$$E = \begin{cases} \frac{\lambda}{2} + \frac{\beta^2}{\lambda} H_x^2 \ \ldots \ \text{two-fold degenerate} \\ -\frac{\lambda}{2} - \frac{\beta^2}{\lambda} H_x^2 \ \ldots \ \text{two-fold degenerate} \end{cases}$$

Substitution in [2] gives

$$\chi_{\perp} = \frac{2N\beta^2}{\lambda} \cdot \frac{e^x - 1}{e^x + 1} .$$

The average susceptibility, then, is given by

$$\overline{\chi} = \frac{N\beta^2}{3kT} \cdot \frac{4x + 4(e^x - 1)}{x(e^x + 1)} \qquad [7]$$

The effective magnetic moment, μ_{eff}, is obtained from the Curie relation

$$\chi = \frac{N}{3kT} \mu_{eff}^2 \quad .$$

Hence

$$\mu_{eff}^2 = \frac{4x + 4(e^x - 1)}{x(e^x + 1)} \text{ in units of } \beta^2 \qquad [8]$$

The limiting values of μ_{eff} under this assumption, then, are:-

1) As $x \to 0$ $(T \to \infty)$, $\mu_{eff} \to 2$.

2) As $x \to \infty$ $(T \to 0)$, $\mu_{eff} \to 0$.

(ii) $\Delta \gg \lambda$, +ve Δ

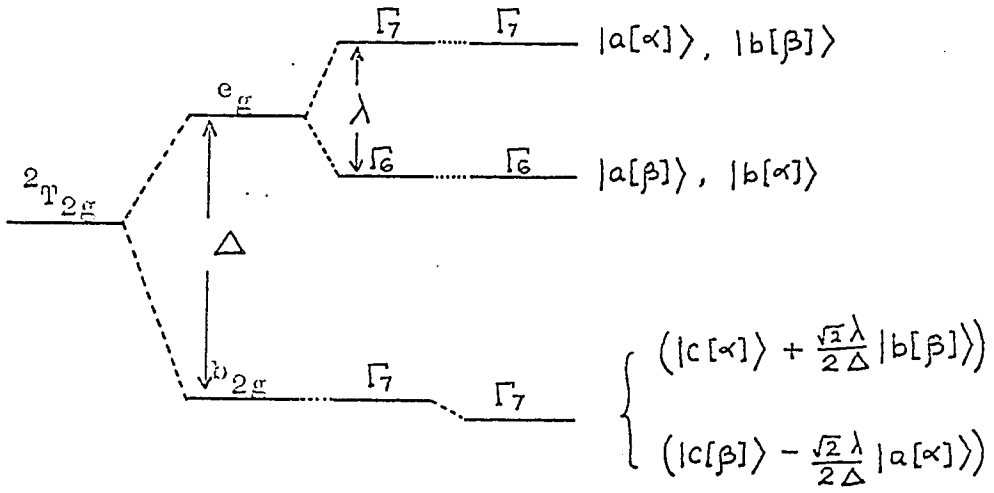

Figure 6. Splitting of $^2T_{2g}$ when $\Delta \gg \lambda$, +ve Δ .

The ground term wave-functions are obtained by mixing $\Gamma_7(e_g)$ into the $\Gamma_7(b_{2g})$ through the spin-orbit coupling since the off-diagonal elements of $\Gamma_7(b_{2g})$ with $\Gamma_7(e_g)$ for $\lambda \hat{l}.\hat{s}$ are

$$\langle e[\beta] | \lambda \hat{l}.\hat{s} | a[\alpha] \rangle = \sqrt{\tfrac{1}{2}}\lambda = -\langle e[\alpha] | \lambda \hat{l}.\hat{s} | b[\beta] \rangle .$$

Using these functions the g values for the ground level are

$$g_{\parallel} = 2$$

$$g_{\perp} = 2(1 - \lambda/\Delta).$$

The average susceptibility, $\bar{\chi}$, therefore, is given by

$$\bar{\chi} = \frac{N\beta^2}{3kT}\left[\tfrac{1}{3}(1 - \frac{2\lambda}{3\Delta}) + 3kT\alpha\right]$$

where α is the sum of the high frequency contributions from the Γ_6 and $\Gamma_7(e_g)$ levels. For the evaluation of α the zeroth order functions for the $\Gamma_7(b_{2g})$ level may be used, in which case

$$\alpha_{\parallel} = 0$$

$$\alpha_{\perp} = 4/\Delta ,$$

neglecting terms containing Δ^2 or higher orders of Δ.

Then $\bar{\alpha} = (1/3)(8/\Delta)$.

Hence

$$\bar{\chi} = \frac{N\beta^2}{3kT}\left[\tfrac{1}{3}(1 - \frac{2\lambda}{3\Delta}) + \frac{8}{\Delta} kT\right]$$

and $$\mu^2_{eff} = \tfrac{1}{3}(1 - \frac{2\lambda}{3\Delta}) + \frac{8}{\Delta} kT \qquad [9]$$

Thus when Δ becomes very large with respect to kT and λ, and only then, the effective moment, μ_{eff}, becomes independent of temperature and acquires the spin-only value of 1.73 B.M.

for example, when $\Delta = 10\lambda$, ignoring the high frequency contribution, $\mu_{eff} = 1.67$ B.M., still somewhat below the spin-only value.

So far the orbital reduction factor k has been omitted, for simplicity. The effect of k is readily deduced from the interpretation given on page 16; as k increases the orbital contribution to the magnetic moment is increased. Hence decreasing k would tend to bring μ_{eff} closer to the spin-only value.

The general case was treated by Figgis (34) by solving the secular equation for the perturbation

$$\mathcal{H}' = (z^2 - r^2/3) + \lambda\hat{l}.\hat{s} + \beta H(k\hat{l} + 2\hat{s})$$

using the functions of $\Gamma_6(e_g)$, $\Gamma_7(e_g)$ and $\Gamma_7(b_{2g})$ listed in figure (4), and substituting the eigenvalues obtained into formula [2]. The results have been expressed by plots of μ_{eff} against $kT/|\lambda|$ for different values of k and $v = \Delta/\lambda$. The following general conclusions are drawn from the results:-

1) The effect on μ_{eff} is small unless Δ is about equal to, or greater than, λ.

2) For higher axial components, μ_{eff} tends towards the spin-only value.

3) The factor k has quite a marked effect on μ_{eff}.

(b) Available Magnetic Data

Since both the strong and the weak-field cases of d^1 lead to the same ground term, $^2T_{2g}$, in octahedral symmetry,

It would be instructive to include a very brief survey, at least, of the data on the first row transition metals. On the whole the number of complexes with the d^1 configuration, especially those of the second and third row, whose magnetic properties have been studied in detail is small; most of the work on the $^2T_{2g}$ term has been on the $(t_{2g})^5$ configuration (35).

(i) First Row Transition Metals

Ti(III), V(IV), Cr(V) and Mn(VI) all form compounds, but the only compounds of hexavalent manganese contain the manganate ion, $MnO_4^{=}$, where the stereochemistry of the manganese ion is tetrahedral. The values of λ for Ti(III), V(IV) and Cr(V) in the free ion, together with the expected values of μ_{eff} at 300°K from Lotani's theory are given below.

	λ free-ion (cm^{-1})	μ_{eff} 300°K
Ti^{+++}	155	1.86 B.M.
V^{4+}	250	1.7 "
Cr^{5+}	380	1.5 "

From Owen (18) and Mitchell and Williams (36) the λ values for the complexes are expected to be somewhat lower. The presence of an axial component in the field would bring the μ_{eff} closer to the spin-only value.

For titanium complexes the present data (20,37-39) seem to require an axial field splitting several times λ; the moments at 300°K are generally between 1.5 and 1.75 B.M.

For V(IV) most of the compounds studied do not have stereochemistries which are even nominally cubic and, therefore, interpretation becomes difficult. From studies by Clark et al. (40) and Clark (41,42) theoretical explanation of the data calls for the introduction of k and Δ; in particular,

	k	Δ
VCl_4(Bipyridyl)	0.95	1100 cm^{-1}
VCl_4(o-phenanthroline)	0.65	750 " .

Very few compounds of Cr(V) are even nominally octahedral. Their moments are generally much closer to 1.73 than to 1.3. $CrOCl_5^=$ is formally octahedral, and the moments for M_2CrOCl_5 are 1.69 at 295°K for M = Rb (20) and 1.60 at 300°K for M = Cs (43).

(ii) Second and Third Row Transition Metals

The magnetic data available for those compounds which are at least formally octahedral are given in table I. The spin-orbit coupling constants for these ions are large; they vary from 750 cm^{-1} for Nb(IV) to about 4000 cm^{-1} for Re(VI). The room temperature moments are, therefore, expected to be somewhat lower than the spin-only value. However, table I shows that most of the compounds of Mo(V) and W(V) have such high moments that it is necessary to assume a low symmetry component so large that the theory, as outlined in an earlier section, is unlikely to remain valid. For those few

Table I

Magnetic Properties of some Hexacoordinated Nb(IV), Ta(IV), Mo(V), W(V) and Re(VI) Compounds

Compound	μ_{eff}(B.M.) at ~300°K	θ°K	Temp. Range (°K)	Ref.
$NbCl_4$-$(Py)_2$	1.37		77 - 298	44
$NbBr_4$-$(Py)_2$ green	1.26		"	"
" red	1.58		"	"
NbI_4-$(Py)_2$	1.05		"	"
$(PyH)_2Nb(OMe)Cl_5$	1.57	61	77 - 299	20
$(QH)_2Nb(OEt)Cl_5$	1.66	19	"	"
$(QH)_2Nb(OPr^s)Cl_5$	1.70	20	"	"
$TaCl_4$-$(Py)_2$	0.69		77 - 298	45
$TaBr_4$-$(Py)_2$	0.43		"	"
$NaMoF_6$	1.66	218	80 - 300	47
K "	1.51	66	"	"
Rb "	1.75	158	"	"
Cs "	1.66	224	"	"
K_2MoOCl_5	1.74	27	90 - 300	48
Rb_2 "	1.69	16	"	49
Cs_2 "	1.65	-10	"	43
$(NH_4)_2$ "	2.12	15	"	20
$(NH_4)_2$ "	1.71	32	"	48
$(PyH)_2$ "	1.74	15	"	"
$(QH)_2$ "	1.74	4	"	"

table I, continued

$(NH_4)_2MoOBr_5$	1.72	51	90 - 300	48
$(PyH)_2$ "	1.82	17	"	"
$(QH)_2$ "	1.80	6	"	"
$NaWF_6$	antiferro-magnetic with Neél point:	125°K	"	47
K "		120	"	"
Rb "		105	"	"
Cs "		105	"	"
Et_4NWCl_6		100	80 - 300	50
Cs "		105	"	"
Me_4N "		140	"	"
Rb_2WOCl_5	1.55	20	100 - 300	49
Cs_2 "	1.49	16	"	"
Cs_2 "	1.56	-30	"	43
$(Me_3NH)_2WOCl_5$	1.35	4	"	49
Cs_2WOBr_5	1.35	17	"	"
ReF_6	0.51		14 - 296	20
$ReCl_6$	2.07	50	98 - 300	53
$(NH_4)_2ReO_2Cl_4.SO_2Cl_2$	2.03	-184	"	54

Measured at room temperature only

$NbCl_4$-$(Py)_2$	1.53	46
" -(γ-picoline)$_2$	1.18	"
" -Bipy	1.06	"
" -o-phen	1.05	"

table I, continued

$NbBr_4$-$(Py)_2$	1.36	46
" -(γ-picoline)$_2$	1.29	"
$TaCl_4$-$(Py)_2$	1.31	"
" -(γ-picoline)$_2$	0.77	"
" -Bipy	0.70	"
" -o-phen	0.67	"
$TaBr_4$-$(Py)_2$	1.02	"
" -(γ-picoline)$_2$	0.77	"
Cs_2MoOCl_5	1.72	49
$(Me\ NH_3)_2$ "	1.74	"
$(Me_2NH_2)_2$ "	1.72	"
$(QH)_2$ "	1.70	"
Rb_2MoOBr_5	1.73	"
Cs_2 "	1.73	"
$(PyH)_2$ "	1.67	"
$MoOCl_3(Ph_3PO)_2$	1.70	20
" $(Ph_3AsO)_2$	1.74	"
" $(Me_2SO)_2$	1.64	"
" $(Me_2CO)(Ph_3AsO)$	1.73	"
$MoCl_5(Ph_3AsO)$	1.6	"
$NaWCl_6$	0.88	51
K "	1.02	"
Rb "	0.88,0.94	"
Cs "	1.17,1.00,1.10	"

table I, continued

$WCl_5(Ph_4As)$	1.21	51
Et_4NWBr_6	1.28	52
$EtNH_3$ "	1.23	"
Rb_2WOBr_5	1.37	49
$KReOF_5$	~1.4	20
Rb "	~1.4	"
Cs "	~1.4	"

Py = pyridine

Q = quinoline

Bipy = 2,2'-Bipyridyl

O-phen= ortho-Phenanthroline

Me = methyl

Et = ethyl

Pr^s = secondary-propyl

Ph = phenyl

other compounds, in which the axial component of the field is not expected to be too large, their moments seem to be consistent with the theory.

EXPERIMENTAL

A. Susceptibility Measurement

When an element of a material (dm) is placed in an inhomogeneous magnetic field (H), it experiences a force (dF) along the field gradient (dH/dx): the force being given by

$$dF = H \chi_g dm(dH/dx)$$

where χ_g is the gram susceptibility.

The Gouy method of measuring susceptibility, employed in this work, involves the measurement of the force integrated over a large difference in the field gradient. The theoretical development of the method has been given in many texts (55,3,56); the final result being the formula

$$10^6 \chi_g = \frac{2lg}{wH^2}(F - \delta) \qquad [10]$$

where l = length of specimen in cm.

w = weight of specimen in gram

H = the field strength in oersted

F = force on sample tube + specimen in mgm.

δ = force on sample tube in mgm.

g = acceleration due to gravity

and χ_g is in c.g.s. units,

provided the sample is contained in an evacuated sample tube with uniform cross-sectional area over the whole length, l,

and the specimen extends far enough from the pole pieces of the magnet that the field at the top of the sample is virtually zero.

(e) The Magnetic Balance

The field (H) was provided by an electromagnet, with a pole gap of 2.0 cms., mounted on an adjustable platform capable of being moved horizontally in two perpendicular directions. Measurements were made at four different field strengths corresponding to the currents of 2.5, 5.0, 7.5 and 10.0 amperes. The current was adjusted and kept constant at any required value by an automatic control unit constructed at the Electrical Engineering Department of this University. The current was measured with a Tech-Simpson Ltd. Model 9, double range ammeter having an accuracy of ±0.5%, full scale.

The force (F) was measured by a damped Sartorius microbalance (MPE 5). The sample was suspended from the left hand pan of the balance by means of a system of brass stirrups, a turnbuckle and a piece of quartz fibre. To guard against draught the sample and the system of quartz fibre, turnbuckle, and stirrupswere enclosed in a jacket detachable at a point below the platform of the balance. The bottom end of the jacket consisted of a piece of copper tubing 7.5 cms. long cemented onto the glass by means of epoxy resin (figure 7). This provided a reasonably uniform temperature throughout the length of the sample (temperature gradient $< 0.5^{\circ}$).

The sample tube was constructed of pyrex glass with an outer diameter of 4 mm. and an inner diameter of 2.5 mm., about 9 cm. long. The top end was joined to a bigger tube (outer diameter = 5 mm.) about 2.5 cm. long to facilitate joining the sample tube to the filling system. It was suspended from a glass hook (see figure 7). For each measurement the sample tube was evacuated and sealed. The following adjustments were made before each measurement:-

(i) The hook was carefully made so that the sample tube was suspended vertically.

(ii) By means of the turnbuckle the bottom end of the sample was adjusted to be exactly at the level of the centres of the pole pieces.

(iii) By means of the adjustable platform the electromagnet was adjusted so as to place the sample tube exactly in the centre of the pole gap.

For measurements at temperatures below room temperature and down to 90°K the sample was cooled by a flow of nitrogen vapour from a liquid nitrogen boiler. Various temperatures in the range 90 - 300°K could be obtained by varying the rate of flow of the nitrogen. This was done by a system of two heaters. To obtain a given temperature a 300 watt heater was first adjusted to give a temperature just above that required. Another heater, having about 1/20th the power of the former, connected to a Thermoelectric Corp. feed-back relay system, provided the extra power to cool the

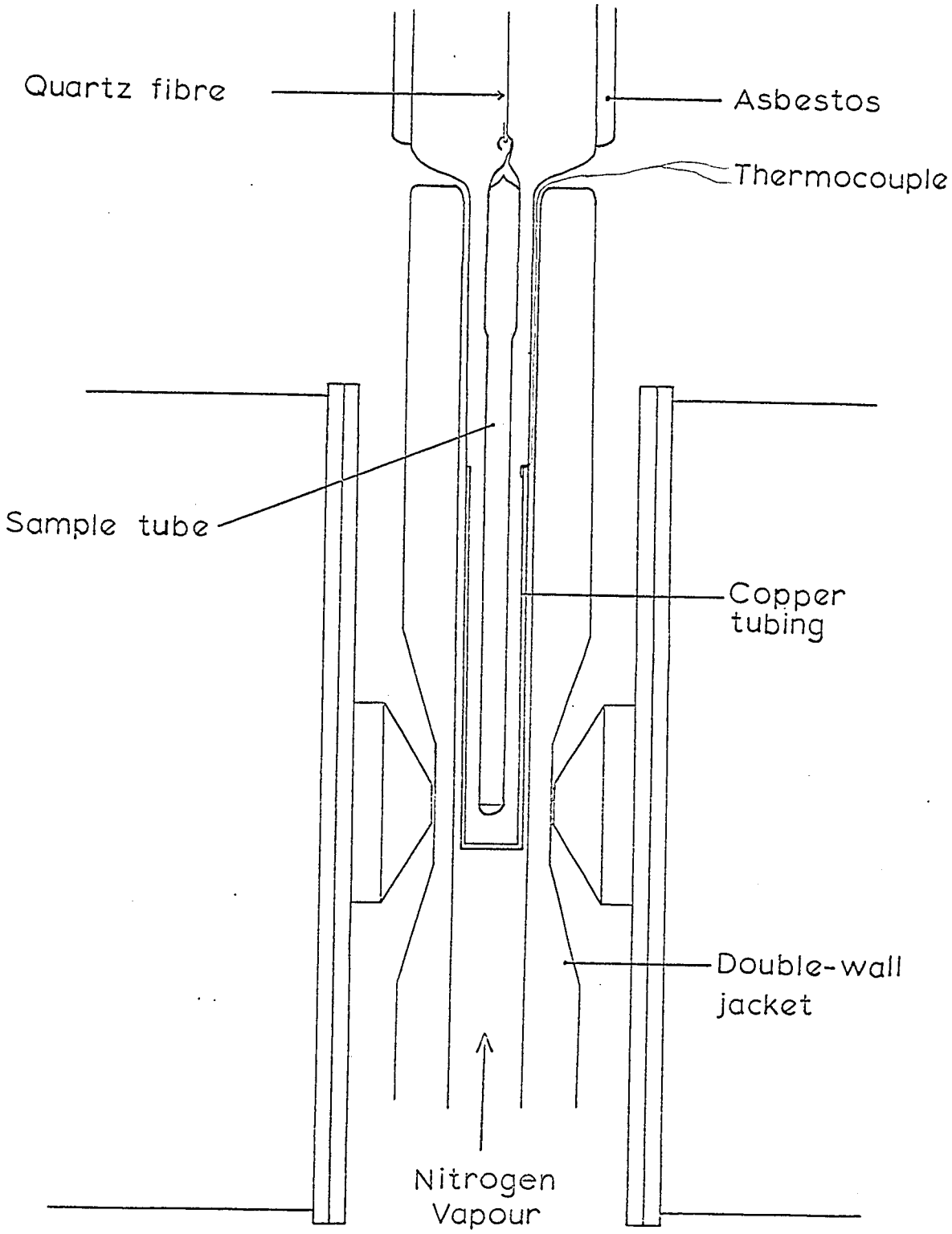

Figure 7. Sample Tube in Position for Measurement

system further to the required temperature and maintain it. The temperature could be kept constant at any value for over 30 minutes, the length of time depended on the rate with which the liquid nitrogen in the boiler (5 litres capacity) was being used up.

The temperature was measured by a thermoelectric Minimite bridge, custom constructed to read down to -200°C using a copper-constantan thermocouple, the operating junction of which was fixed on the inside of the jacket at about the middle of the sample. Figure (7) shows a section of the assembly in operation at the pole gap of the electro-magnet. The Minimite-thermocouple system was calibrated at 0°C, -78°C and -183°C; a correction of up to -3°C was found necessary on the Minimite readings at -183°C, but decreasing to zero at room temperature.

(b) Sample Tube Correction (δ)

Since glass is diamagnetic the force observed on the empty sample tube (δ) is negative. From each reading on a sample the appropriate value of δ at the same temperature had to be subtracted. The values of δ at various temperatures were determined by measuring the apparent change of the weight of the evacuated tube alone when the magnetic field was applied. The absolute value of δ increased with decreasing temperature, as can be seen from figure (8). These

Figure 8. Sample Tube Correction for Tube No. 1

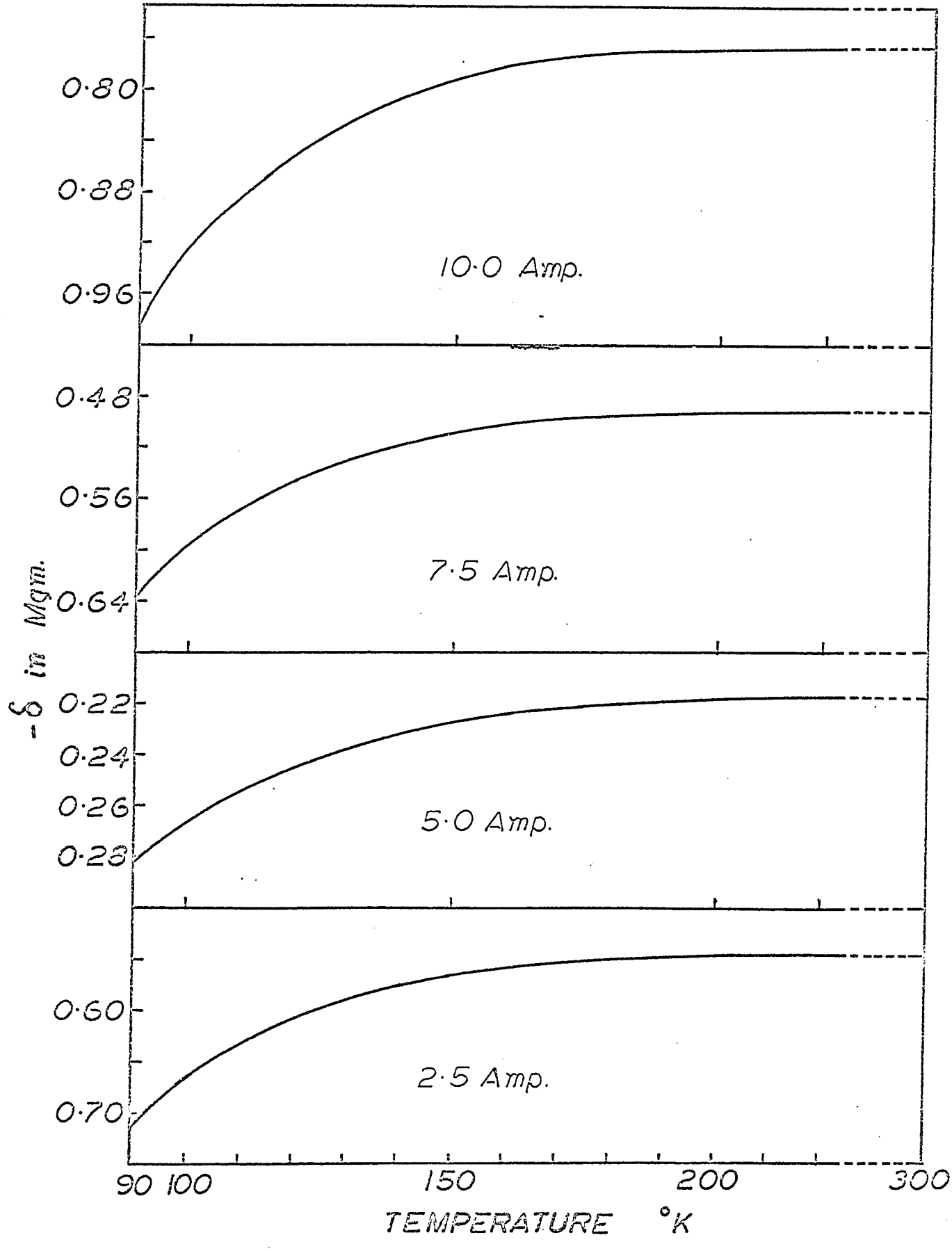

curves were used to read off values of δ at any temperature for any given current. It should be pointed out here that the correction for each sample tube had to be determined separately.

(c) Calibration of the Field (H)

From formula [10] it is apparent that H can be calculated if χ_g is known, and vice versa. In practice the Gouy balance is usually calibrated with a substance of known susceptibility rather than by measuring the field directly. In the present work the apparatus was calibrated with $HgCo(CNS)_4$, the suitability test, properties and preparation of which have been given by Nyholm and Figgis (57,58). It has a gram susceptibility of $(16.44 \pm 0.08) \times 10^{-6}$ c.g.s. units at 20°C, and obeys the Curie-Weiss law with $\theta = 10^{0}$ over the range room temperature to 80°K.

The measurements on $HgCo(CNS)_4$ were taken at several temperatures between room temperature and 90°K. The results are shown in table II. Formula [10] was used to calculate H^2/g.

(d) Measurement of Samples

Each sample to be measured was first carefully ground. Some of the powder was then introduced into the sample tube, and the tube tapped about one hundred times; a little more was then added, tapped; the process was repeated until a

Table II

Field Strengths at various Currents

Current (Amp.)	Temp. (^{o}K)	H^2/g	Mean H^2/g	H (Oersted)
2.5	299	1.8178	1.816	1335
	269.5	1.7841		
	231.5	1.8173		
	191	1.8400		
	141	1.8191		
5.0	299	7.0993	7.070	2630
	269.5	7.0592		
	231.5	7.0574		
	191	7.0221		
	141	7.1108		
7.5	299	15.4756	15.62	3920
	269.5	15.6049		
	231.5	15.6903		
	191	15.6167		
	141	15.7309		
10.0	299	23.8828	23.96	4850
	269.5	23.7688		
	231.5	24.1313		
	191	23.8533		
	141	24.1633		

column of powder 6 to 9 cm. long was obtained. Such meticulous steps were followed in the packing of the tube in order to ensure a reasonably uniform packing for all samples. For compounds which were air-sensitive (all except $Hg[Co(CNS)_4]$) these operations were carried out under nitrogen. The system was then connected to a vacuum line, evacuated, and the sample tube sealed.

For each sample measurements were carried out at room temperature, 273°K, 253°K and so on at 20 degree intervals down to 90°K. The sample was then allowed to warm up to room temperature and measurements at this temperature repeated to check if any irreversible change had occurred. In all cases the two sets of measurements at room temperature coincided within experimental error. After the correct setting of the control unit for a desired temperature was obtained the system was allowed from 15 to 30 minutes to attain a steady thermal state before measurement at that temperature was begun.

For each field strength the apparent weights together with the rest points before and after the field was applied were recorded three or four times. This procedure was necessary particularly for the low temperatures and high field, in both cases a significant drift of the rest points occurred.

The gram susceptibility, χ_g, was calculated using formula [10] for each field strength. A plot of χ_g against 1/H indicated whether there was any ferromagnetic impurity in the sample. In most cases (see later section) the plots gave lines parallel to the 1/H axis, indicating that the samples were essentially free from such impurity.

In a few cases the samples were mixtures of the complex (paramagnetic) and the tetrahalide (diamagnetic). For these, χ_g for the paramagnetic complex was calculated by using Klodemann's additivity law:

$$\chi = \chi_1 m_1 + \chi_2 m_2 \qquad [11]$$

where χ is the experimental value,

χ_1, χ_2 are the susceptibilities of the components having the mole fractions m_1 and m_2 respectively.

The molar susceptibility χ_M was calculated from

$$\chi_M = \chi_g \times \text{Molecular Weight},$$

and the effective magnetic moment, μ_{eff}, was obtained from the relation

$$\mu_{eff} = 2.84(\chi'_M T)^{\frac{1}{2}}$$

where $\chi'_M = \chi_M$ - Diamagnetic Correction.

The diamagnetic correction includes contributions from the ligands as well as from the core of the paramagnetic ion, i.e. Nb(IV) and Ta(IV).

(e) Precision and Accuracy of Measurements

Since χ_g was calculated from equation [10] its accuracy depends upon the accuracy with which l, w, F and H^2 could be determined.

The length of the sample was between 8 and 9 cm. and it could be measured to 0.1%. The weight w, was normally between 0.3 and 0.5 gm., and it could be determined with an accuracy better than 0.05%.

The error in H^2 can be calculated from the figures in table II. The mean deviation for H^2/g for the four currents varies from 0.4 to 0.6%.

The force F encountered in the measurements of the various samples varied from 0.050 mgm. to 1.0 mgm. The mean deviation calculated from a series of four readings at each current setting for the various samples varies from 1.5% for the low values to 0.1% for the largest force measured.

Hence the accuracy of the reported values of χ_g is at best 0.8% and at worst about 2-3%. The error due to non-uniformity of packing of the samples is not accounted for in this estimate. However, Figgis and Nyholm (57) reported satisfactory reproducibility if special care is taken in the packing procedure.

B. Preparation of Samples

Tetrahalides of Niobium and Tantalum

The preparations of the tetrahalides were carried out in two steps from the metals. The metals were first halogenated to give the pentahalides, which were then reduced to the tetrahalides by some fresh metal. These two steps were carried out in a single system, thus avoiding transference from one system to another at any stage.

Chlorination of the metal (M_1) was achieved by passing dried chlorine gas from a cylinder over heated metal. Bromination was carried out by heating the metal (M_1) with vapours of bromine at the vapour pressure of the liquid held at room temperature. Reagent grade bromine (Allied Chemicals) was dried over well out-gassed P_2O_5 overnight under vacuum and then vacuum-distilled into the reaction tube.

The reduction of the pentahalide by the metal (M_2) was achieved by placing the reaction tube in a temperature gradient. These procedures were modifications of those described by McCarley and Torp (44), McCarley and Boatman (43) and Schäfer and Kahlenberg (59). Table IV summarizes the conditions for these preparations and figure (9) gives diagrams of the reaction tubes.

Figure 9. Reaction Tubes for the Preparation of Tetrahalides

(a) Tetrachloride

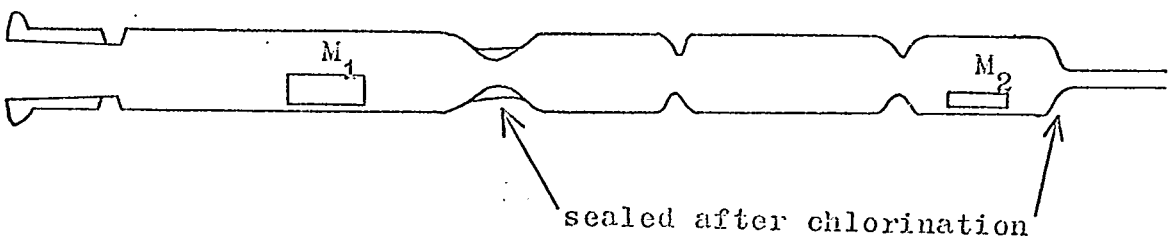

(b) Tetrabromide

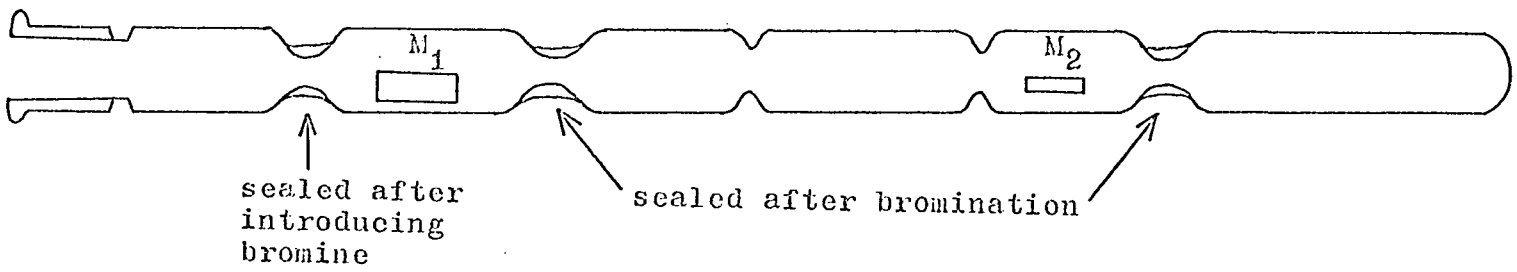

Material: pyrex for niobium
quartz for tantalum

The temperature gradient was obtained by placing two aluminium block furnaces end to end, one set for the higher temperature and the other for the lower.

The products were transferred to storage ampoules in a dry box and stored under nitrogen.

Table III

Typical Analyses of Tetrahalides

Compound	% Metal		% Halogen	
	Found	Calc.	Found	Calc.
$NbCl_4$	40.09	39.59	60.03	60.41
$NbBr_4$	22.77	22.52	77.27	77.48
$TaCl_4$	56.41	56.05	44.13	43.95
$TaBr_4$	36.50	36.14	63.74	63.86

Table IV

Conditions for the Preparation of Tetrahalides

Final Product	Halogenation Temp. in °C	Reduction of MX_5 Temp. Grad. (M/MX_5) in °C
$NbCl_4$	230	365/235
$NbBr_4$	400	415/350
$TaCl_4$	300	685/255
$TaBr_4$	375	630/300

Complexes of $NbCl_4$, $NbBr_4$, $TaCl_4$ and $TaBr_4$ with Pyridine, and 2,2'-Bipyridyl/N,N,N',N'-Tetramethylethylenediamine

The procedure for the preparation of the complexes is as below, the conditions for each individual complex being given in Table V.

Carefully dried sulphur-free benzene was further dried under vacuum over fresh sodium overnight in a suitable distillation apparatus fitted to a Schlenk tube. About 30 mls. was then vacuum-distilled into the Schlenk tube by cooling the latter in ice-water, and then dry nitrogen was admitted into the system. The tetrahalide (about 2 gm.) was then introduced and the suspension stirred until most of the crystals were broken down to fine powder (about 5 hours). The purified ligand (calculated to give 25 - 50% excess) was then added to the suspension. Reaction with the powdered tetrahalide was usually rapid; however, stirring was continued for an extended period of time (table V) before the solid material obtained was separated in a filtering apparatus similar to that described by Fritz et al.(60). The product was washed with two or three volumes of benzene, dried by pumping at 40 - 50°C for 10 to 20 hours and stored in sealed ampoules under nitrogen.

Pyridine (Baker Analysed Reagent) was dried over sodium hydroxide pellets and then distilled. 2,2'-bipyridyl

Table V

Preparation of the Complexes of Tetravalent Nb and Ta

Reactants			Wt. of MX_4	Period of stirring	Colour of Product
$NbCl_4$	+	Pyridine	1.15 gm.	$5\frac{1}{2}$ days	light brown
$NbCl_4$	+	2,2'-bipyridyl	1.05 "	24 hours	blue
$NbCl_4$	+	4meen*	1.45 "	18 "	pink
$NbBr_4$	+	Pyridine	1.50 "	24 "	green
$NbBr_4$	+	2,2'-bipyridyl	1.60 "	23 "	dark green
$NbBr_4$	+	4meen*	1.75 "	30 "	olive
$TaCl_4$	+	Pyridine	1.30 "	48 "	brick red
$TaCl_4$	+	2,2'-bipyridyl	1.60 "	28 "	dull green
$TaCl_4$	+	4meen*	1.25 "	46 "	grey
$TaBr_4$	+	Pyridine	1.20 "	50 "	chocolate
$TaBr_4$	+	2,2'-bipyridyl	1.69 "	4 days	green
$TaBr_4$	+	4meen*	1.90 "	59 hours	light purple

* 4meen=N,N,N',N'-tetramethylethylenediamine

(Fisher Reagent) was sublimed under reduced pressure. N,N,N',N'-tetramethylethylenediamine (Aldrich) was fractionally distilled under reduced pressure, collecting the fraction boiling between 88 and 89°C (at 50 mm. pressure).

C. Analysis of Samples

The analyses of niobium and tantalum in the tetrahalides and the complexes were done gravimetrically: a sample in a tared crucible was moistened with water, oxidized with a few drops of conc. HNO_3 and ignited in a muffle furnace to constant weight at 1100°C.

The chlorine and the bromine contents were determined by Volhard titration. The tetrahalides were first dissolved in sodium hydroxide solution, oxidized with hydrogen peroxide and then neutralized with nitric acid and distilled ammonia. For the complexes the sample was prepared by the Parr bomb fusion technique prior to titration.

Carbon, hydrogen and nitrogen were analysed by Schwarzkopf Microanalytical Laboratory, New York. The process of preparing the samples for these analyses involved the use of dry-box technique. Therefore, it is assumed that the analytical data for carbon, hydrogen and nitrogen are less reliable than those for the halogen and the metal. Hence the composition of those samples which were mixtures was calculated from the data for bromine and metal only (table VII).

Table VI

Analytical Data of the Complexes

Complex	% Calculated					% Found				
	M	X	C	H	N	M	X	C	H	N
$NbCl_4$-$(Py)_2$	23.64	30.09	30.57	2.57		23.77	36.43	30.60	2.81	
$NbCl_4$-Bipy	23.77	36.28	30.73	2.06		23.42	36.37	32.29	2.39	
$NbCl_4$-4meen	26.47	40.41	20.54	4.60		26.24	40.61	21.07	4.79	
$NbBr_4$-$(Py)_2$	16.28	56.00	21.04	1.77		15.96	55.28	22.27	2.20	
*$NbBr_4$-Bipy	16.34	56.20	21.12	1.42		17.11	58.55	20.67	1.67	
$NbBr_4$-4meen	17.57	60.45	13.63	3.05		17.43	59.68	14.90	3.43	
$TaCl_4$-$(Py)_2$	37.62	29.48	24.97	2.09		37.86	29.44	25.16	2.27	
$TaCl_4$-Bipy	37.78	29.61	25.08	1.68		37.90	29.58	26.64	2.12	
$TaCl_4$-4meen	41.22	32.31	16.42	3.67		41.47	32.57	17.39	4.39	
*$TaBr_4$-$(Py)_2$	27.47	48.52	18.23	1.53		28.04	50.08	18.00	1.82	
*$TaBr_4$-Bipy	27.55	48.67	18.29	1.23		28.37	50.24	18.65	1.44	
*$TaBr_4$-4meen	29.34	51.82	11.68	2.61	4.54	29.78	52.52	12.00	2.66	4.34

* mixtures (see table VII for composition); M = metal; X = halogen

These samples were assumed to be mixtures of the complex and the tetrahalide only. Attempts to obtain pure samples by prolonging the period of stirring for these cases were not successful.

Table VII

Composition of Impure Samples

Sample	Composition	
	% Complex	% Tetrahalide
$NbBr_4$-Bipy	88.3	11.7
$TaBr_4$-$(Py)_2$	91.6	8.4
$TaBr_4$-Bipy	90.1	9.9
$TaBr_4$-4meen	94.1	5.9

RESULTS AND DISCUSSION

Tetrahalides and Ligands

The susceptibilities of the tetrahalides and the ligands are given in table VIII. Measurements on the tetrahalides were taken at five temperatures from room temperature to 100°K. For $NbBr_4$, $TaCl_4$ and $TaBr_4$, plots of χ_g versus 1/T showed a slight curvature indicating the presence of traces of ferromagnetic impurities; the values of χ_g, the mean values of which are given in the table, are those extrapolated to infinite field.

Table VIII

Susceptibilities of Tetrahalides and Ligands

Compound	Mean $\chi_g \times 10^6$ (c.g.s.)	Mean $\chi_M \times 10^6$ (c.g.s.)	Ref.
$NbCl_4$	-0.187	-43.8	
$NbBr_4$	-0.188	-77.5	
$TaCl_4$	-0.178	-57.5	
$TaBr_4$	-0.183	-91.4	
Pyridine	-0.623	-49.3	61
2,2'-Dipyridyl		-105	3
4mpen		-94	3

Symmetry of the Ligand Field

Conductivity measurements by McCarley (44) and infra-red spectra obtained by Allbutt et al. (46) indicated that the pyridine complexes probably have octahedral coordination. The infra-red spectrum of the analogous compound $TiCl_4(py)_2$ suggests a cis- rather than a trans- configuration (62). A similar arrangement is likely for the niobium and the tantalum compounds. Hence all the complexes in this work, MX_4L_2, where L_2 = $(py)_2$, bipy. and bmeen, belong to the same symmetry group, viz. C_{2v}. However, since the electronic structure of a complex is determined only by the sum of the charges on each axis, if all distances are equal (Ballhausen (6), page 107), these complexes can be regarded as having D_{4h} symmetry. This is, no doubt, an approximation, but from the visible spectra and magnetic properties of the complexes of vanadium (IV) with 2,2'-bipyridyl and o-phenanthroline (42), and from the absorption spectra of NbX_4(acetonitrile)$_2$ (X = Cl,Br,I) (63), it seems to be a fairly good one to make. The complexes of NbX_4 and TaX_4 (X = Cl,Br) with pyridine, 2,2'-bipyridyl and tetramethylethylenediamine are therefore considered to be cases of tetragonally distorted octahedra in the discussion which follows.

Complexes of Niobium

Tables IX and X give the results of the susceptibility measurements on the complexes of niobium.

Table IX

Results of Magnetic Measurements on the Complexes of $NbCl_4$

Complex	Temp. (^oK)	$\chi_g \times 10^6$ (c.g.s.)	$1/\chi'_M \times 10^{-2}$	μ_{eff} (B.M.)
$NbCl_4$-$(Py)_2$	296.5	1.80	11.8	1.43
	273	2.96	11.0	1.42
	252	2.15	10.1	1.42
	232	2.35	9.38	1.41
	209.5	2.62	8.53	1.41
	188.5	2.91	7.78	1.40
	170.5	3.23	7.08	1.39
	151.5	3.71	6.25	1.40
	131	4.30	5.46	1.39
	111	5.11	4.65	1.39
	92	6.20	3.88	1.38
$NbCl_4$-Bipy	300	1.70	12.3	1.40
	250	2.01	10.7	1.37
	210	2.37	9.30	1.35
	192.5	2.56	8.70	1.34
	170.5	2.92	7.75	1.33
	161	3.05	7.46	1.32
	142	3.43	6.71	1.31
	132	3.77	6.16	1.31
	125	4.02	5.81	1.32
	110	4.60	5.14	1.31
	98.5	5.26	4.54	1.29
$NbCl_4$-4meen	298	1.05	19.8	1.10
	277	1.11	18.9	1.09
	255	1.18	18.1	1.07
	234	1.28	17.0	1.05
	212	1.38	16.1	1.03
	191.5	1.48	15.2	1.01
	167.5	1.66	13.9	0.99
	146	1.85	12.7	0.96
	127.5	2.06	11.6	0.94
	113	2.23	10.9	0.92
	90	2.83	8.85	0.91

Table X

Results of Magnetic Measurements on the Complexes of $NbBr_4$

Complex	Temp. (^oK)	$\chi_g \times 10^6$ (c.g.s.)	$1/\chi'_M \times 10^{-2}$	μ_{eff} (B.M.)
$NbBr_4$-$(Py)_2$	299	1.17	11.8	1.43
	274	1.27	11.1	1.41
	250.5	1.39	10.3	1.40
	232	1.48	9.79	1.38
	212.5	1.60	9.09	1.37
	193.5	1.74	8.55	1.35
	172.5	1.94	7.80	1.34
	150	2.27	6.70	1.33
	127.5	2.72	5.69	1.33
	112	3.15	5.07	1.34
	92.5	3.83	4.23	1.33
$NbBr_4$-Bipy	300	1.17	11.7	1.43
	253.5	1.33	10.7	1.37
	213.5	1.50	9.64	1.34
	190.5	1.67	8.81	1.32
	171.5	1.80	8.29	1.29
	154	1.97	7.66	1.27
	142	2.12	7.21	1.26
	130.5	2.29	6.73	1.25
	124.5	2.40	6.47	1.25
	114.5	2.56	6.09	1.23
	103	2.77	5.68	1.21
	90	3.18	5.02	1.20
$NbBr_4$-4meen	297.5	0.570	21.2	1.07
	294.5	0.548	21.7	1.05
	273	0.585	20.8	1.03
	253	0.610	20.2	1.00
	232	0.710	18.2	1.01
	211	0.753	17.6	0.98
	192	0.812	16.6	0.96
	171.5	0.855	16.0	0.93
	154	1.01	14.2	0.94
	132	1.14	12.9	0.91
	112	1.365	11.2	0.90
	92	1.625	9.70	0.88

The values of χ_g at all temperatures at which measurements were taken were independent of the field strength for all the six complexes, indicating that the samples were essentially free from any ferromagnetic impurity. For the calculation of χ'_M, the reciprocals of which are given in colum four in tables IX and X, the susceptibility values given in table VIII were used for the diamagnetic correction.

From figures (10) and (11) it is seen that in no case is the Curie-Weiss law strictly obeyed, even though the plot for $NbCl_4(py)_2$ shows only a slight curvature. McCarley and Torp, however, obtained results which fitted the Curie-Weiss relationship over the temperature range 77 - 298°K for the pyridine complexes. The following table shows the comparison of the room temperature moments obtained in this work with those of other workers for some of the complexes.

	this work	McCarley(44)	Allbutt*(46)
$NbCl_4-(py)_2$	1.43 B.M.	1.37 B.M.	1.53 B.M.
$NbBr_4-(py)_2$	1.42 "	1.26 "	1.36 "
$NbCl_4-Bipy$	1.40 "		1.06 "

* measured at room temperature only

From the treatment of the limiting cases when $\Delta \gg \lambda$ (page 22) or from the consideration of the general case by Figgis (34) it is seen that when the tetragonal splitting of the $^2T_{2g}$ term leaves the doublet e_g lowest, the variation of μ_{eff} with temperature differs from that of the octahedral

Figure 10. $1/\chi'_M$ vs. T for Complexes of $NbCl_4$

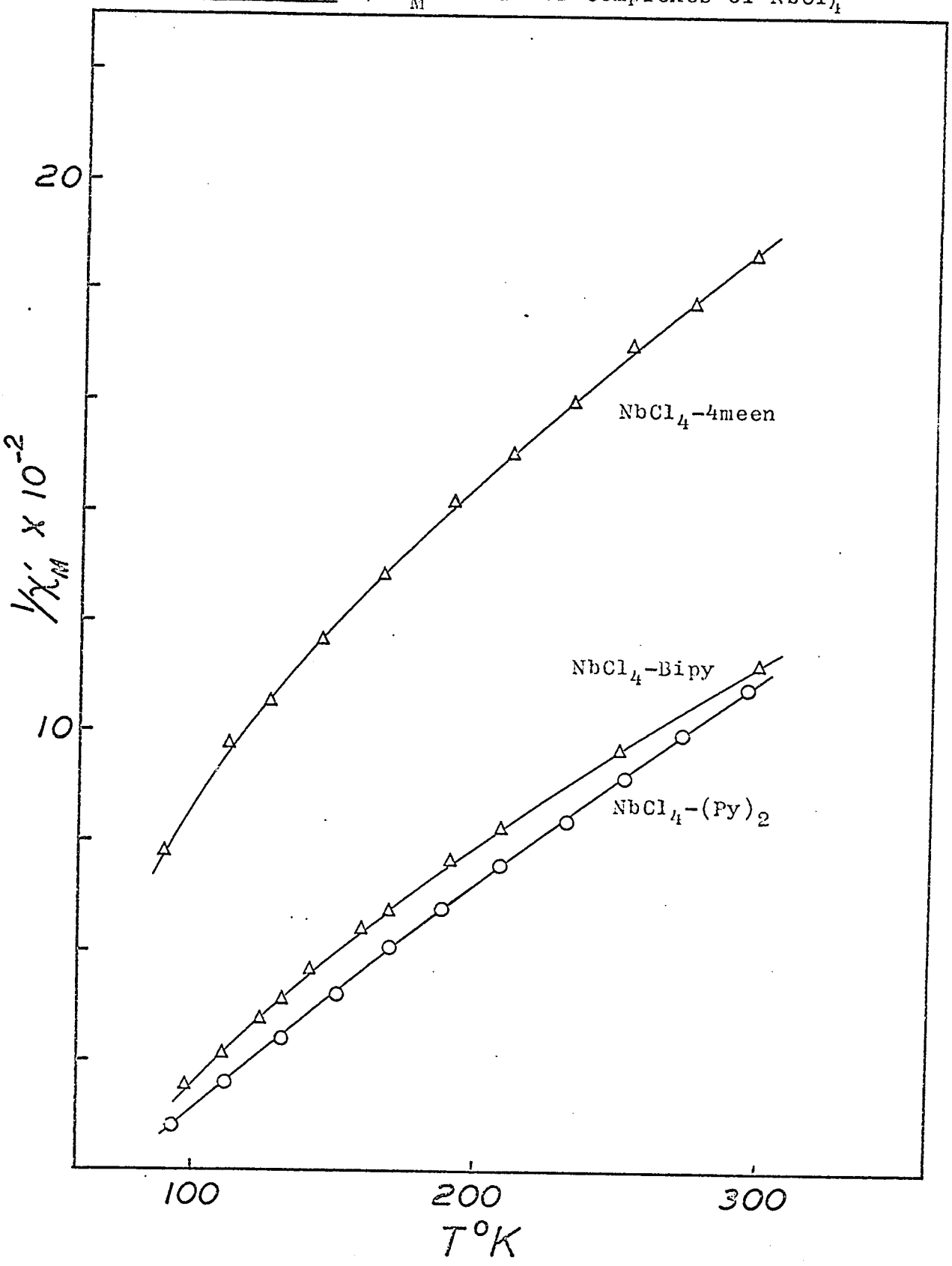

Figure 11. $1/\chi'_M$ vs. T for Complexes of $NbBr_4$

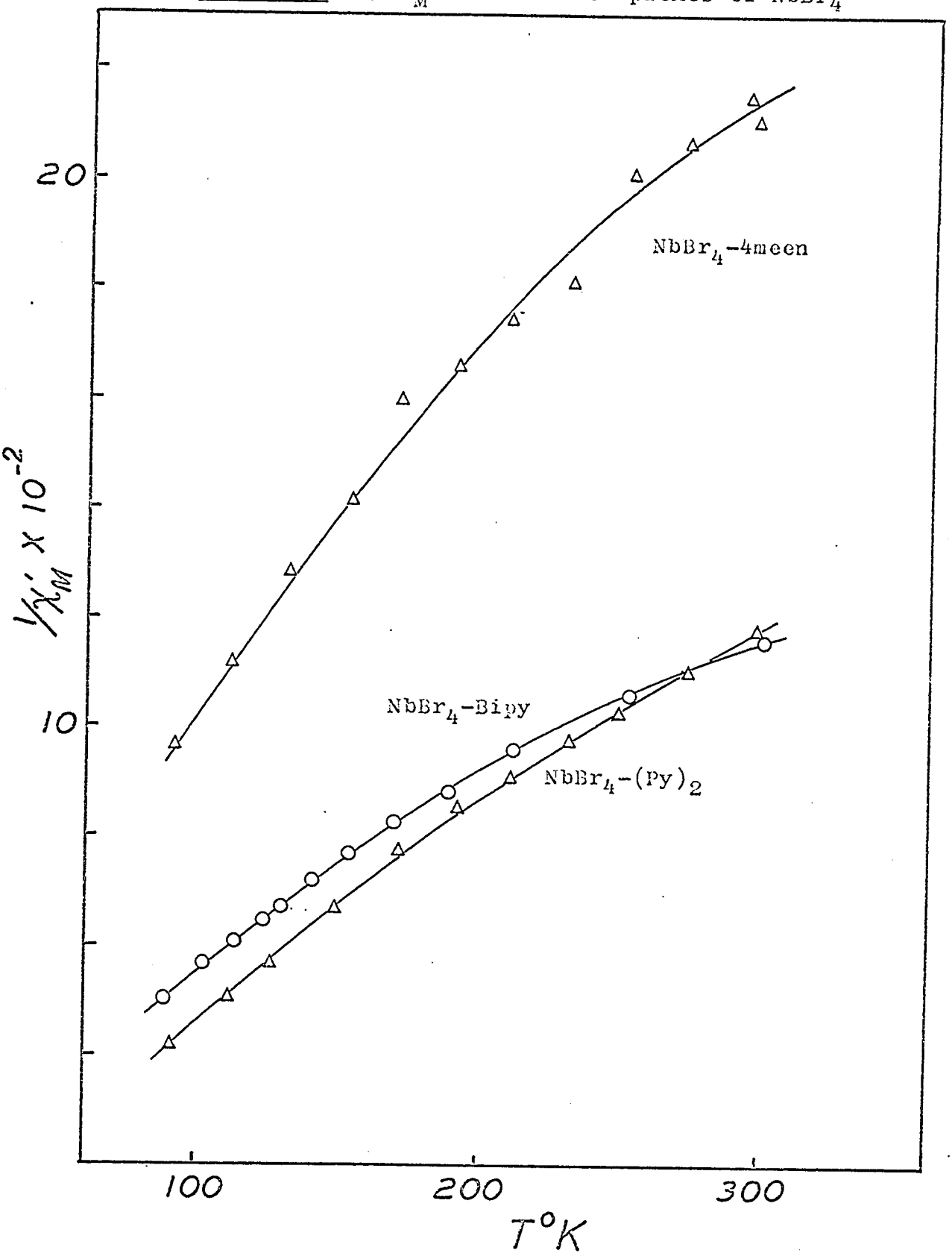

symmetry (Kotani's theory) only slightly: $\mu_{eff} \to 2$ as $T \to \infty$, whereas in the Kotani plot for the d^1 configuration $\mu_{eff} \to \sqrt{5}$ as $T \to \infty$; when $T \to 0$ for both cases $\mu_{eff} \to 0$. The Kotani plot for d^1 and the plot of μ_{eff} against $kT/|\lambda|$ for $v = \Delta/\lambda = \pm 10$ are reproduced in figure (12) from Figgis (34).

The free-ion value for λ for Nb(IV) is 750 cm^{-1} (20,page 99), so that kT/λ varies from 0.08 to 0.3 in the temperature range 90 - 300°K, or if the λ value for the complex is assumed to be decreased by about 30% as was found for the complexes of vanadium (IV) with 2,2'-bipyridyl and o-phenanthroline (42), kT/λ varies from 0.14 to 0.5. By comparing the variation of μ_{eff} with temperature for the complexes of Nb(IV) found here, given in figures (13)-(15), with figure (12) it is found that our results cannot be fitted to the curves in figure (12) with $v = 0$ or negative. Our results seem to suggest that the splitting of the $^2T_{2g}$ term by the tetragonal field is such as to leave the singlet b_{2g} lowest. In this case μ_{eff} tends towards the spin-only value of 1.73 B.M., independent of temperature, as the ratio v tends to infinity (page 25).

The crystal field model of the complex and taking into consideration the order of the ligands in the spectrochemical series — halogen < nitrogen — leads to a prediction of negative Δ, i.e. with e_g lying lowest. As pointed out in an earlier section the nature of the metal-ligand bond affects

Figure 12. μ_{eff} vs. kT/|λ| for d^1 Configuration

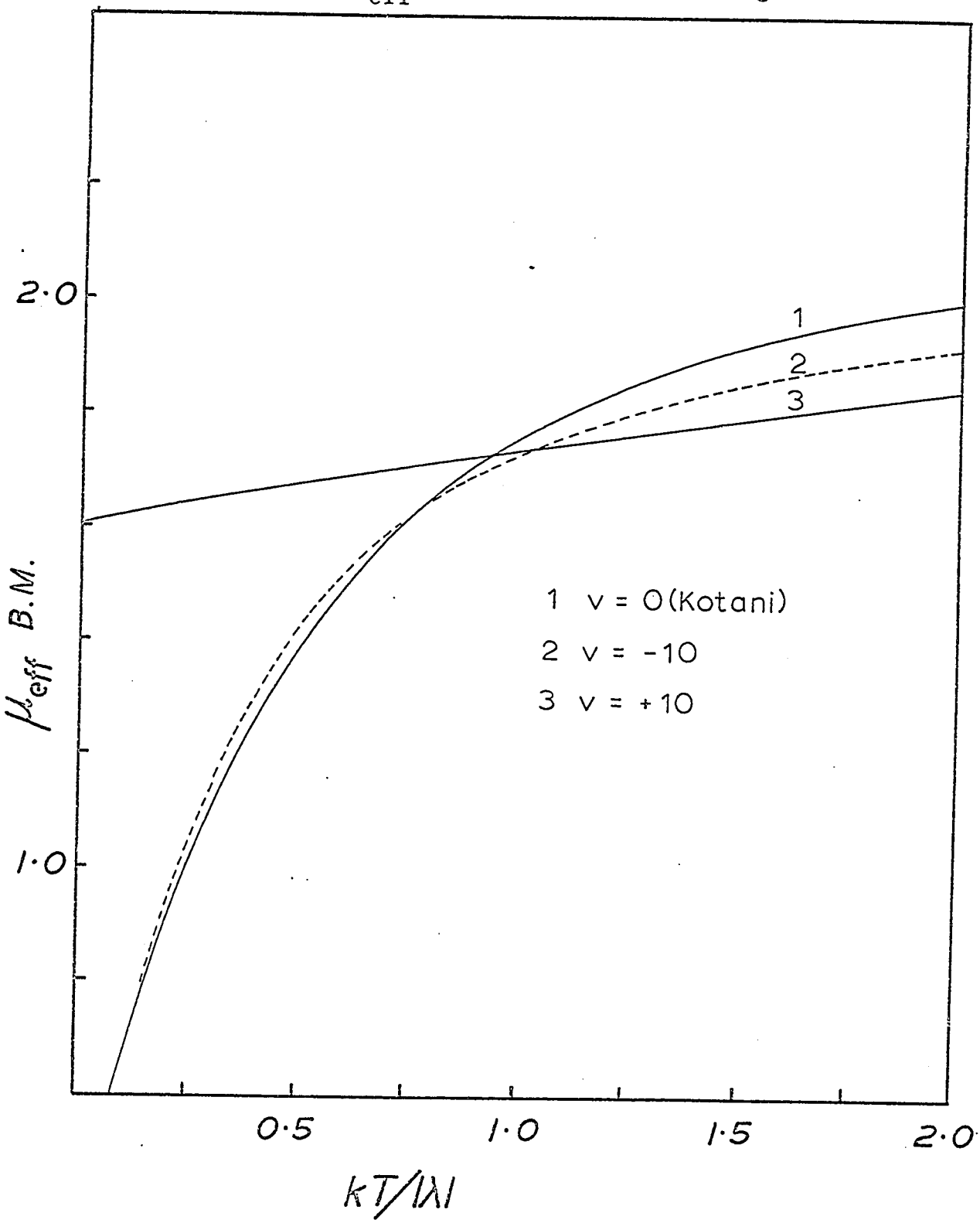

the magnitude of the crystal field splitting 10Dq in octahedral complexes. McClure (64) has discussed this aspect in some detail and he has proposed a two-dimensional spectrochemical series to account for the effects of both the σ- and the π-bond formation. This argument may be extended to the t_{2g} orbitals of the central ion (d_{xy},d_{xz},d_{yz}) in order to explain the reversal in the sign of Δ. Chloride and bromide ions are known to engage in π-bonding which involves their filled p-orbitals and the d-orbitals of the central metal ion, or specifically the d_{xy}, d_{xz} and d_{yz} orbitals. In the case that the d-orbitals are at least partially filled, such bonding destabilizes the t_{2g} orbitals of the metal ion. For the di-substituted cis-complex it is readily seen from the figure below that the d_{xz} and the d_{yz} orbitals can form π-bonds with three halide ions, whereas the d_{xy} orbital can bond with only two (those in the xy-plane). Hence the d_{xz} and the d_{yz} orbitals are destabilized to the same extent, but the increase in the energy of the d_{xy} orbital is somewhat less.

The nitrogen donor ligands pyridine and 2,2'-bipyridyl can also take part in π-bonding with the central metal ion, but the tetramethylethylenediamine cannot. Therefore, it is concluded that the π-donor effect from the halogens alone is sufficient to offset the electrostatic effect and reverse the positions of the $e_g(d_{xz},d_{yz})$ and the $b_{2g}(d_{xy})$ orbitals

Figure 13. μ_{eff} vs. T for $NbCl_4$-$(Py)_2$ and $NbBr_4$-$(Py)_2$

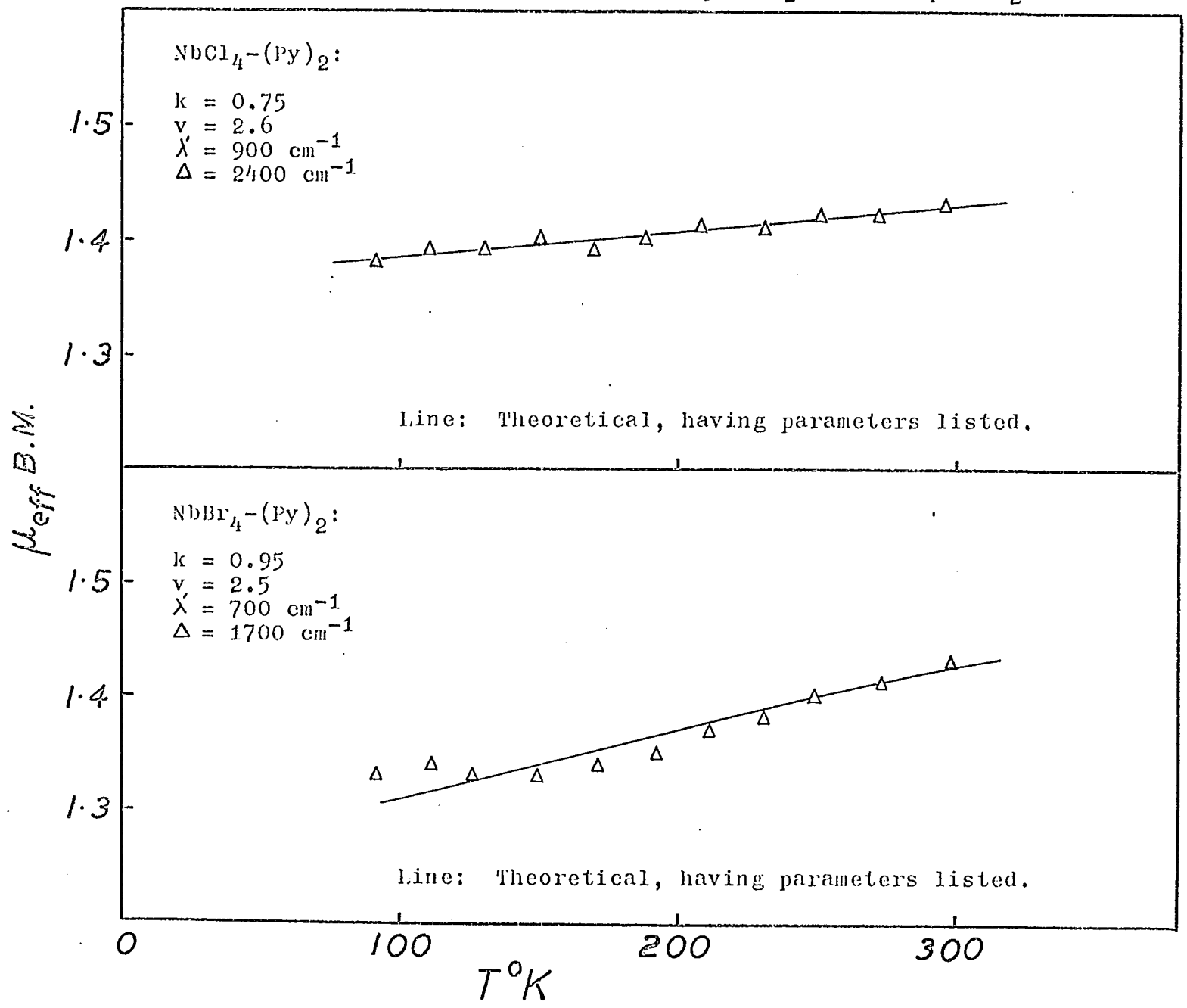

Figure 14. μ_{eff} vs. T for $NbCl_4$-Bipy and $NbCl_4$-4meen

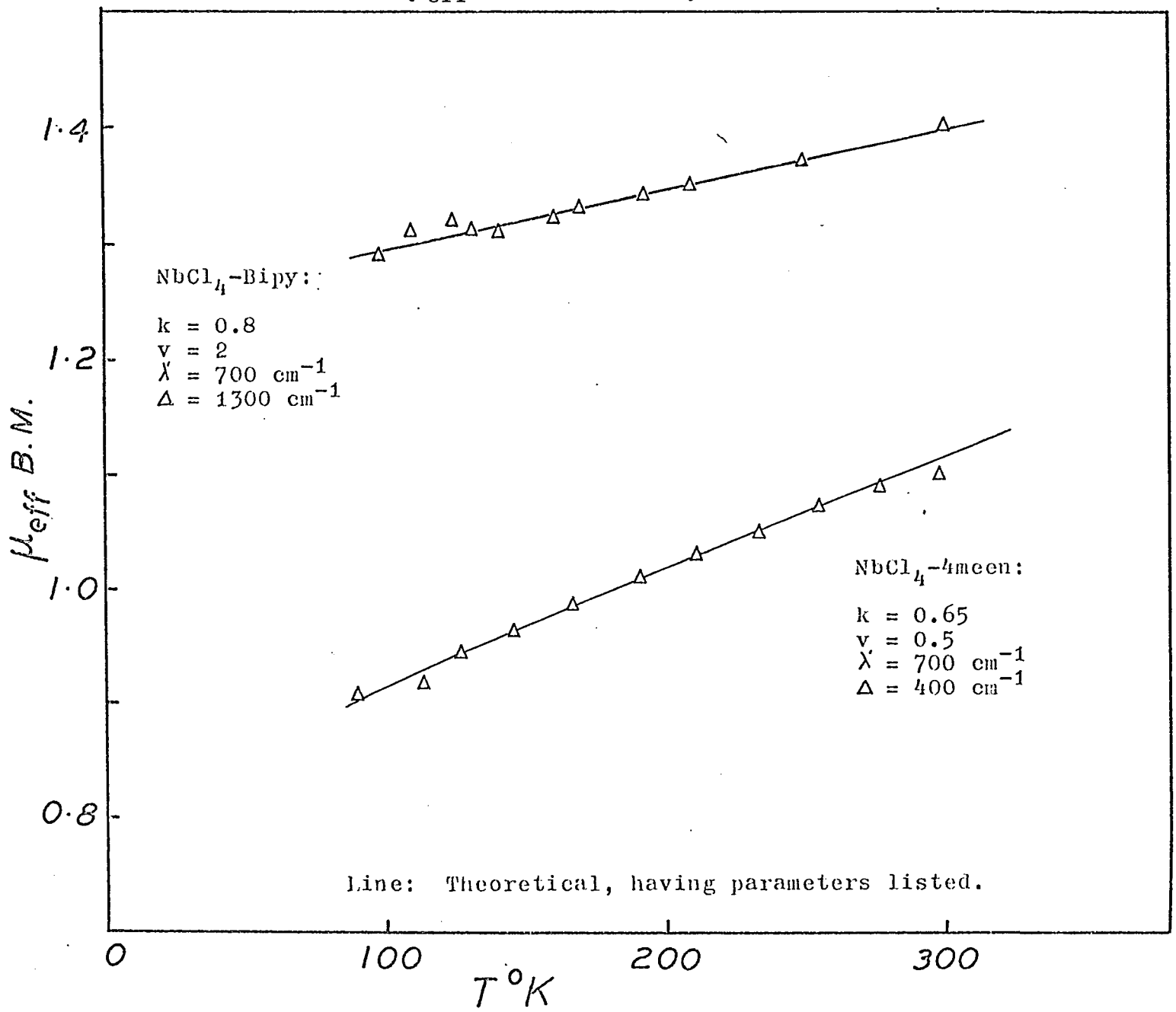

Figure 15. μ_{eff} vs. T for $NbBr_4$-Bipy and $NbBr_4$-4meen

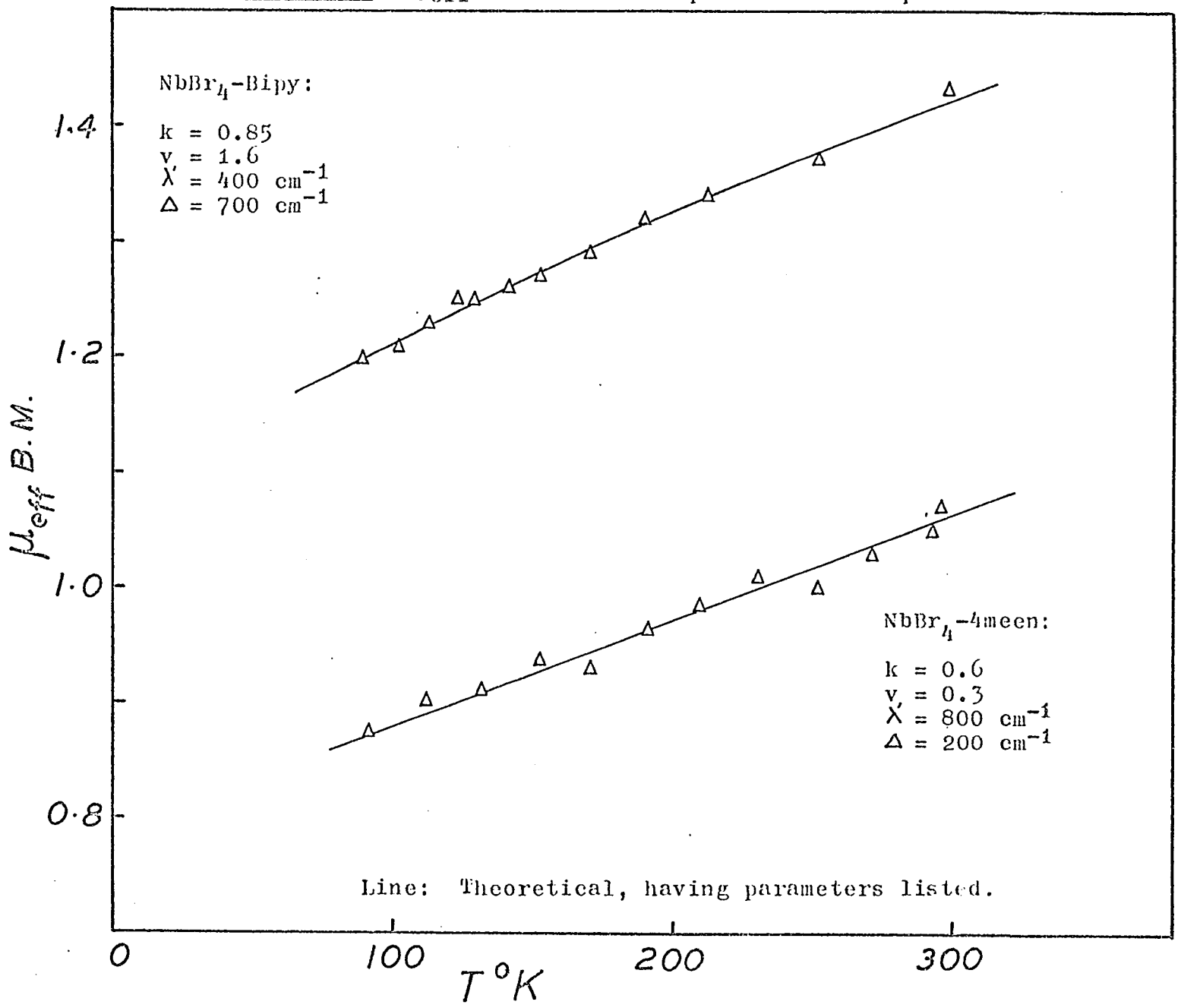

with respect to one another. A similar argument has been suggested by Griffith and Orgel in their spectral studies of chlorocobaltammine complexes (65).

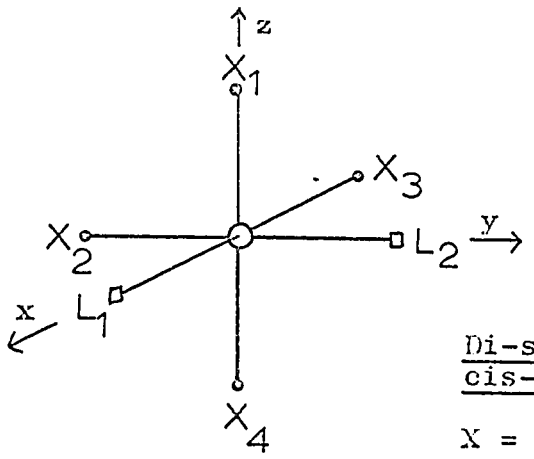

Di-substituted cis-complex

X = halide ion

Tables IX and X also show that the μ_{eff} values for the bromide complexes are lower than those for the corresponding chloride complexes. McCarley and Torp (44) suggested that this difference is due to the greater π-donor capacity of the bromide ions. As the argument requires also that the nitrogen-containing ligands be π-acceptors it cannot explain a similar difference in the complexes with the tetramethylethylenediamine since the latter is not a π-bonding ligand. However, it is a consequence of our deduction above that the difference between the chlorides and the bromides would be determined largely by the order in which they occur in the spectrochemical series. This is because halide ions with a stronger π-donor capacity than the chlorides, say, would merely raise the energy of both the $e_g(d_{xz}, d_{yz})$ and the b_{2g} (d_{xy}) orbitals by approximately the same amount (see figure

21); the difference in the magnitude of Δ must have arisen from (a). Since $Br^- < Cl^-$ in the series, the tetragonal splitting Δ, should be greater for the chlorides as the results show.

Complexes of Tantalum

The results of the magnetic susceptibility measurements of the complexes of tantalum are given in tables XI and XII.

The values of χ_g were found to be slightly dependent on the field strength except for the pyridine complexes. The values listed in column three of tables XI and XII have been corrected for this effect by extrapolating the curves of χ_g against 1/H to infinite field strength. The values of χ'_M are calculated using the diamagnetic susceptibilities given in table VIII.

Here again the plots of $1/\chi'_M$ against T, given in figures (16) and (17), indicate that the Curie-Weiss law is not obeyed in contrast to the results obtained by McCarley and Boatman for the pyridine complexes (43). The free-ion λ for Ta(IV) is about 1500 cm^{-1}, so that kT/λ ranges from 0.04 to 0.14 in the temperature range 90 - 300°K. From figure (12) it is apparent that the μ_{eff} against $kT/|\lambda|$ curve, with μ_{eff} having a value of about 0.4 to 0.7 B.M. (μ_{eff} for the pyridine complexes obtained by McCarley), is very dependent on even small changes in the kT/λ ratio. It is rather

Table XI

Results of Magnetic Measurements on the Complexes of $TaCl_4$

Complex	Temp. (^oK)	$\chi_g \times 10^6$ (c.g.s.)	$1/\chi'_M \times 10^{-2}$	μ_{eff} (B.M.)
$TaCl_4$-$(Py)_2$	298	0.243	36.6	0.81
	248	0.285	34.1	0.77
	213	0.345	31.1	0.74
	189.5	0.390	29.1	0.73
	173.5	0.438	27.3	0.72
	148.5	0.555	23.6	0.71
	141	0.604	22.4	0.71
	124.5	0.680	20.7	0.70
	116.5	0.732	19.7	0.69
	105	0.817	18.2	0.68
	95.5	0.880	17.3	0.67
$TaCl_4$-Bipy	299	0.065	51.6	0.68
	252.5	0.100	47.5	0.66
	209.5	0.170	41.0	0.64
	191	0.215	37.7	0.64
	171.5	0.253	35.2	0.63
	153	0.32	31.7	0.63
	144.5	0.358	29.9	0.62
	134	0.407	28.0	0.62
	124.5	0.440	26.8	0.61
	114	0.510	24.5	0.61
	92.5	0.685	20.3	0.60
$TaCl_4$-4meen	296	0.065	55.6	0.66
	272.5	0.090	52.3	0.65
	250	0.110	50.1	0.64
	230	0.136	47.3	0.63
	208.5	0.170	44.2	0.62
	189.5	0.205	41.4	0.61
	170.5	0.250	39.2	0.60
	150	0.281	36.4	0.58
	132	0.325	34.0	0.56
	124.5	0.364	32.1	0.56
	110	0.390	30.9	0.54
	101	0.462	28.2	0.54
	90	0.516	26.5	0.52

Table XII

Results of Magnetic Measurements on the Complexes of $TaBr_4$

Complex	Temp. (°K)	$\chi_g \times 10^6$ (c.g.s.)	$1/\chi'_M \times 10^{-2}$	μ_{eff} (B.M.)
$TaBr_4$-$(Py)_2$	297	0.144	35.1	0.83
	251	0.168	33.3	0.78
	210	0.195	31.4	0.73
	190.5	0.206	30.7	0.71
	173	0.238	28.8	0.70
	152.5	0.290	26.2	0.68
	143.5	0.287	26.4	0.66
	133	0.323	24.8	0.66
	124.5	0.373	23.0	0.66
	113	0.355	23.6	0.62
	103.5	0.352	23.7	0.59
	90	0.377	22.8	0.56
$TaBr_4$-Bipy	298	0.044	44.4	0.74
	252	0.072	41.0	0.70
	211	0.102	38.0	0.67
	191	0.164	32.9	0.68
	172	0.155	33.5	0.64
	152	0.210	29.9	0.64
	142.5	0.224	29.1	0.63
	132	0.250	27.7	0.62
	124.5	0.290	25.8	0.62
	112	0.341	23.8	0.62
	103	0.372	22.7	0.61
	90	0.496	19.2	0.62
$TaBr_4$-4meen	295	0.052	46.0	0.72
	274	0.068	44.0	0.71
	250.5	0.074	42.3	0.68
	231	0.095	41.2	0.67
	208.5	0.118	38.7	0.66
	187.5	0.133	37.4	0.64
	167.5	0.165	34.8	0.62
	147	0.209	31.8	0.61
	134	0.219	31.2	0.59
	112	0.263	28.8	0.56
	91	0.316	26.3	0.53

surprising, therefore, that the results of McCarley fitted the Curie-Weiss plot as this gives μ_{eff} independent of temperature. Our results show a small dependence of μ_{eff} on temperature (figures 18 - 20).

The room temperature moments for the pyridine complexes of $TaCl_4$ and $TaBr_4$ and of $TaCl_4$-bipy are available in the literature for comparison with those obtained here.

	this work	McCarley (45)	Allbutt* (46)
$TaCl_4$-$(Py)_2$	0.80 B.M.	0.69 B.M.	1.37 B.M.
$TaBr_4$-$(Py)_2$	0.82 "	0.43 "	1.02 "
$TaCl_4$-bipy	0.67 "		0.70 "

* measured at one temperature only

The results obtained by Allbutt and co-workers for μ_{eff} of $TaCl_4$-$(py)_2$ (and perhaps that of the bromide analogue as well) seem to be too high. Our values seem to be consistent with those of the niobium analogue, in that there is a small difference in the μ_{eff} between the pyridine and the bipyridyl complexes.

Analysis of μ_{eff} against T Plots

In figures (13) - (15) and (18) - (20) the lines are curves of μ_{eff} against $kT/|\lambda|$ chosen from the data listed in (34), by empirical methods, to fit the experimental results (represented by points). From these lines of best-fit the values of the parameters k, v, λ', and Δ are obtained for each complex: these are listed in table XIII.

Figure 16. $1/\chi'_M$ vs. T for Complexes of $TaCl_4$

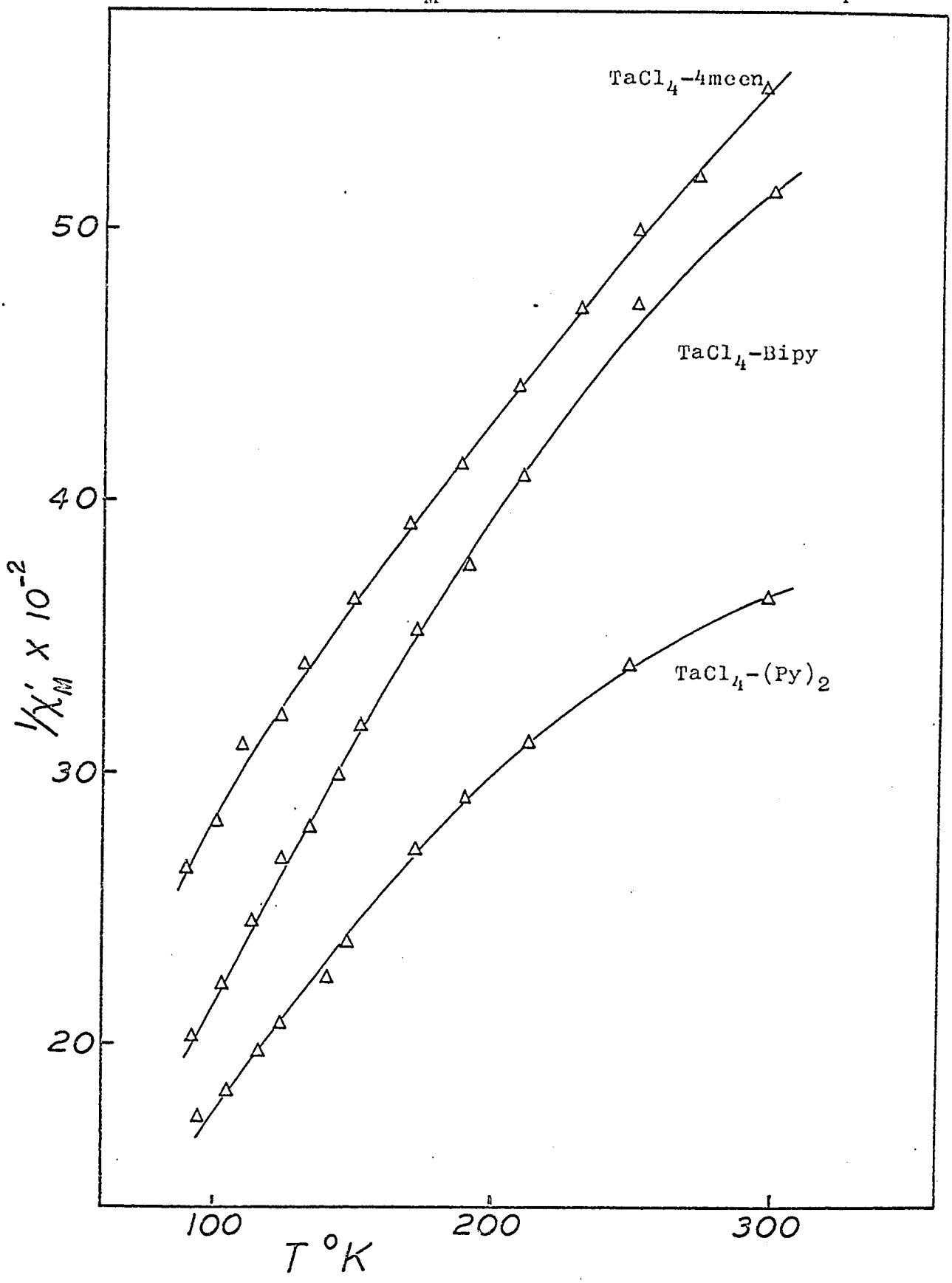

Figure 17. $1/\chi'_M$ vs. T for Complexes of $TaBr_4$

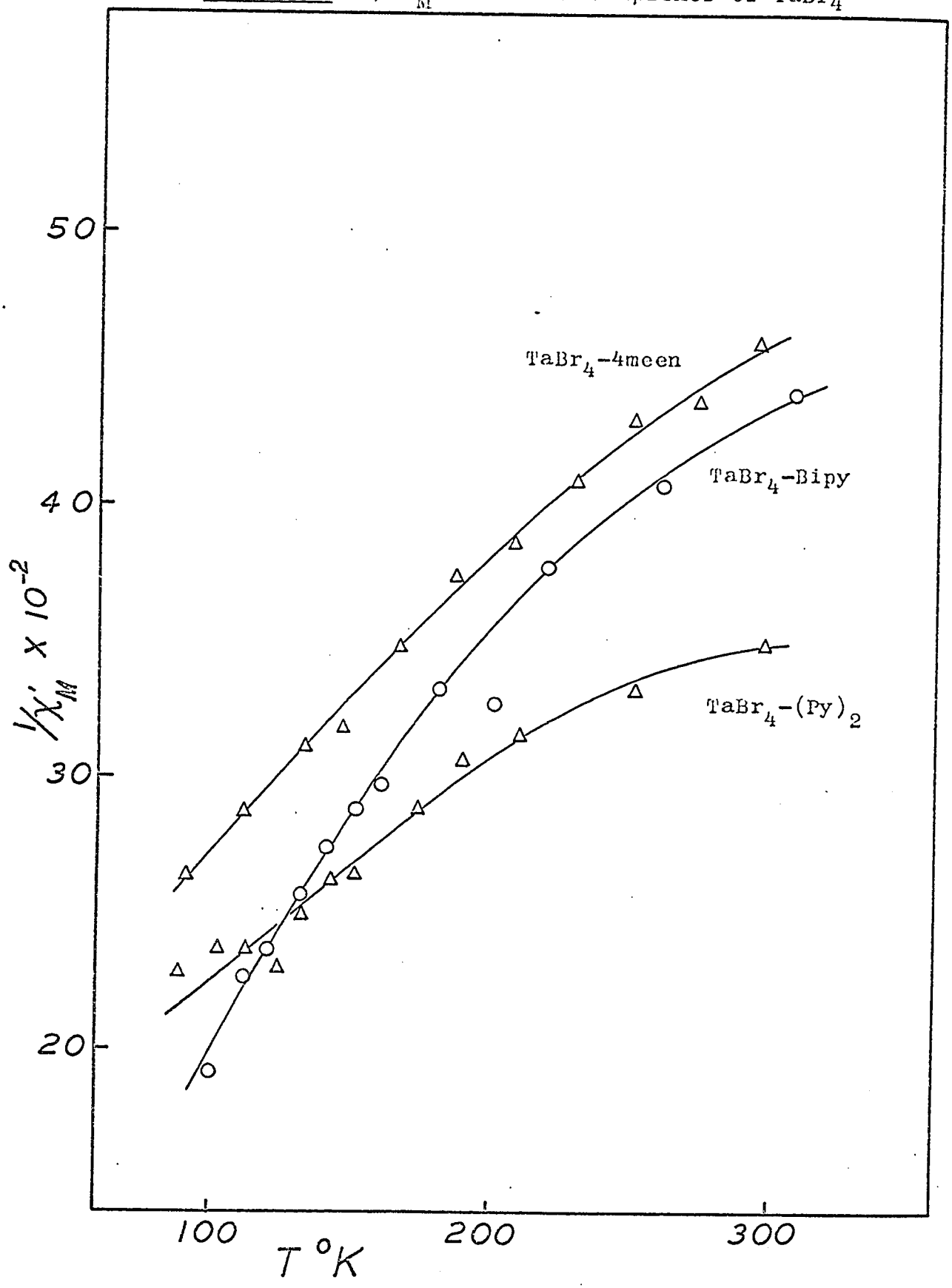

Table XIII

Values of k, v, λ' and Δ obtained by empirical fitting of Figgis's Theory

Complex	k	v	$\lambda'(cm^{-1})$	$\Delta(cm^{-1})$
$NbCl_4$-$(Py)_2$	0.75	2.6	900	2400
" -Bipy	0.8	2	700	1300
" -4meen	0.65	0.5	700	400
$NbBr_4$-$(Py)_2$	0.95	2.5	700	1700
" -Bipy	0.85	1.6	400	700
" -4meen	0.6	0.3	800	200
$TaCl_4$-$(Py)_2$	0.7	0.25	1900	500
" -Bipy	0.65	0.05	3500	180
" -4meen	0.7	0	2300	---
$TaBr_4$-$(Py)_2$	0.8	0.25	1500	400
" -Bipy	0.7	0.1	2000	200
" -4meen	0.8	0.2	1900	400

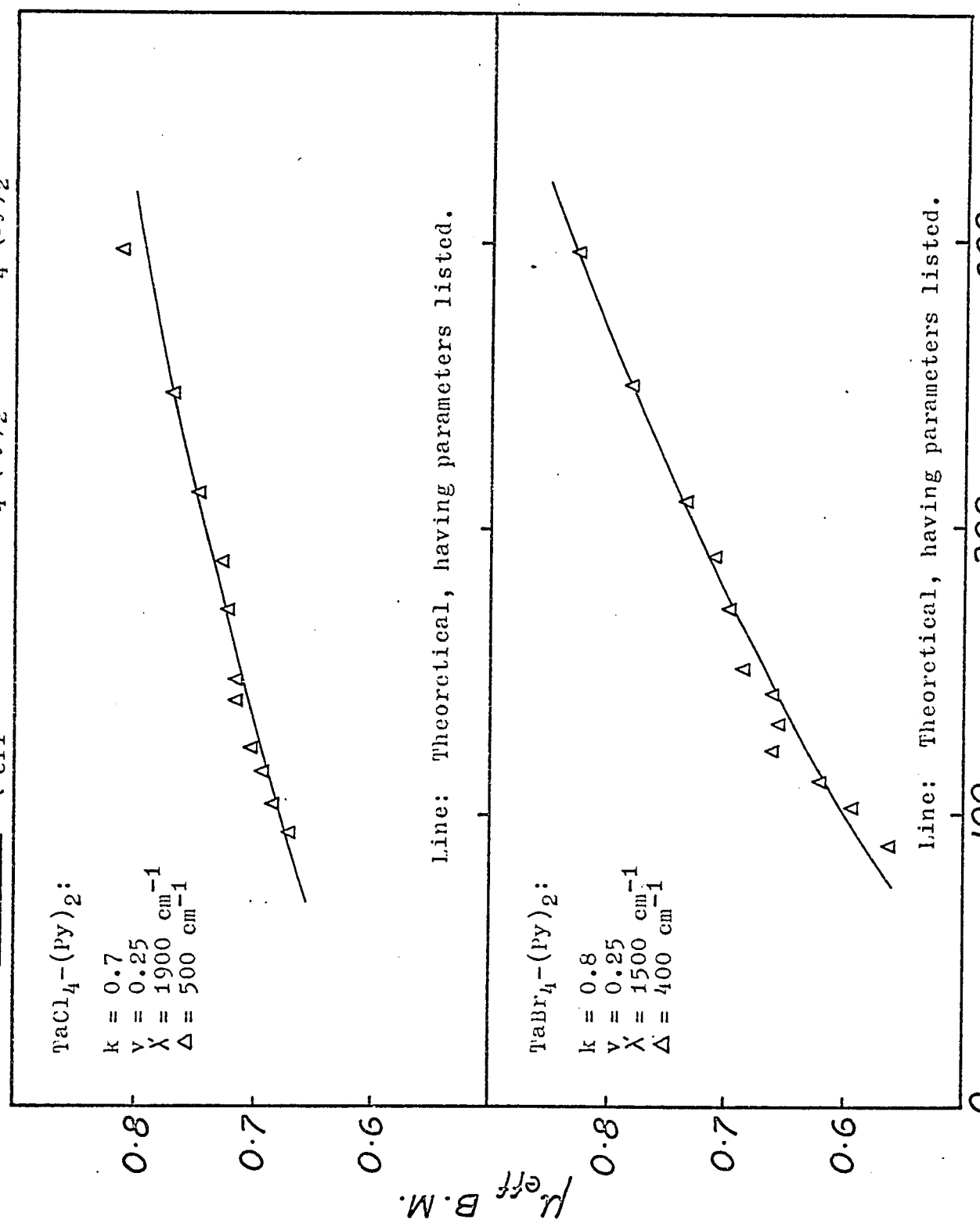

Figure 18. μ_{eff} vs. T for $TaCl_4$-(Py)$_2$ and $TaBr_4$-(Py)$_2$

Figure 19. μ_{eff} vs. T for $TaCl_4$-Bipy and $TaBr_4$-Bipy

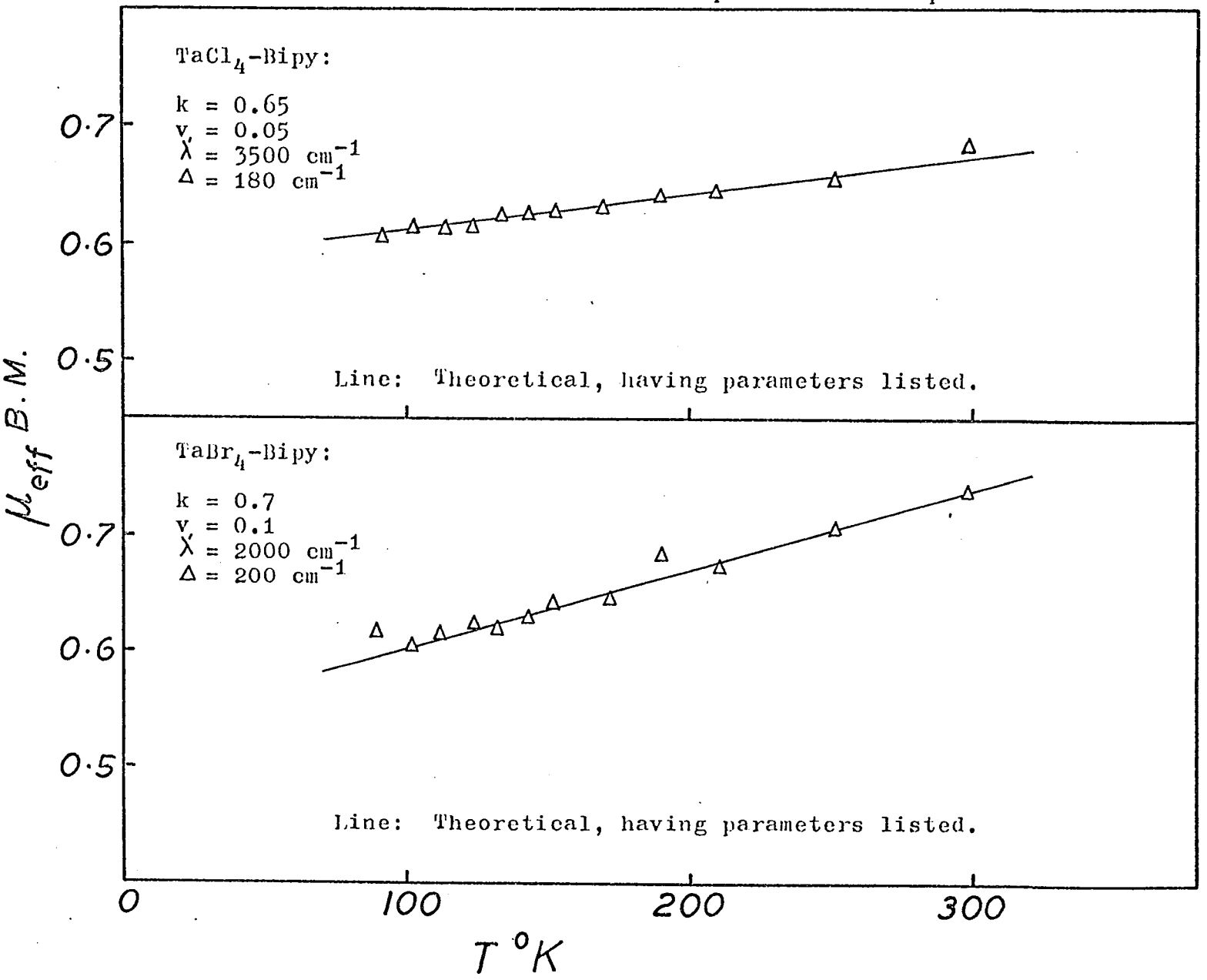

Figure 20. μ_{eff} vs. T for $TaCl_4$-4meen and $TaBr_4$-4meen

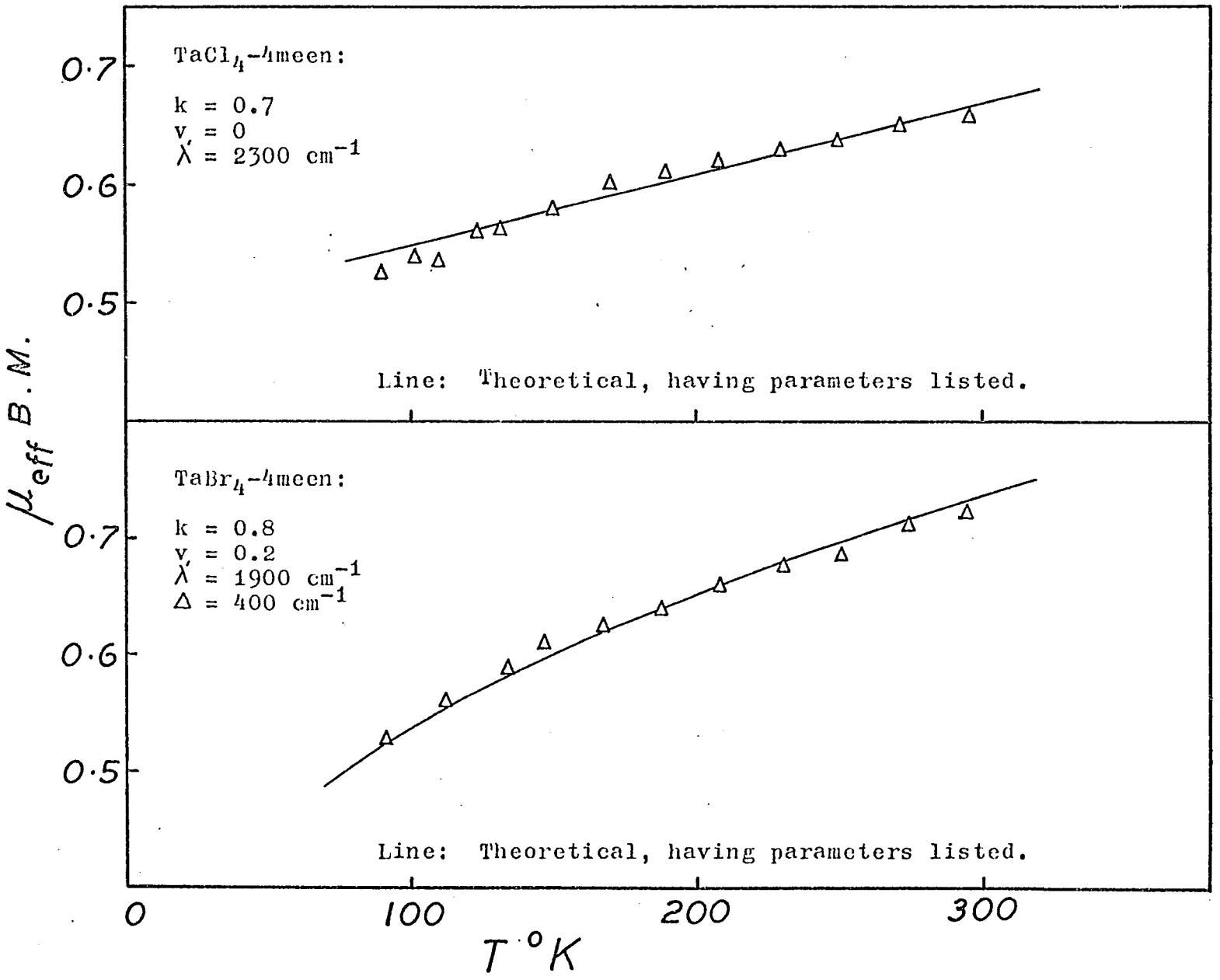

The curve fitting process is rather sensitive, as was shown by Figgis (35); small displacements of the curves give rather marked differences in the parameters obtained. Figgis has also estimated the error in these parameters. They are rather large: λ' values are probably ±30% and the Δ values are subject to an error of about ±50%.

The λ' values for the niobium complexes obtained above seem reasonable since the free-ion value for Nb(IV) is 750 cm^{-1}, but those obtained for the tantalum complexes appear to be too high (free-ion value is probably 1000 - 1500 cm^{-1}). One reason for these poor results could be the inapplicability of the theory for $\Delta/\lambda < 1$. Figgis evaluated the energies by using those functions of the various levels derived under the assumption that the axial field perturbation is greater than the spin-orbit perturbation (i.e. $\Delta/\lambda > 1$ at least). From figures (4) and (5) it is seen that when λ is larger than Δ, the wave functions are different. A second reason may be that the low moments of tantalum (IV) complexes are not fully accounted for by the high spin-orbit coupling, as has been assumed up to date. Superexchange may well be occurring.

Table XIII shows the values of Δ for the complexes with the three nitrogen donor ligands. It is seen that Δ decreases in the order pyridine > bipyridyl > 4ween. It has been discussed in an earlier section that π-donation from the halide ions probably plays a significant role in these complexes

and that it alone can reverse the sign of Δ from that expected on the basis of the crystal field model. It is, therefore, tempting to attribute the above order in the values of Δ to the difference in the degree with which the nitrogen donor ligands affect the π-donating capacity of the halide ions in their respective complexes. The nitrogen in tertiary aliphatic amine is more basic than the nitrogen in aromatic systems such as pyridine. Thus in the complexes with tetramethylethylenediamine, because of the greater σ-donor capacity of the latter (compared to the aromatic ligands), the π-donating capacity of the halide ions may be somewhat inhibited. This effect would produce a smaller difference in the energies of the $e_g(d_{xz}, d_{yz})$ and the $b_{2g}(d_{xy})$ levels as shown in figure (21). It is also implied in the diagram that the tetramethylethylenediamine produces a larger splitting at (a) and this enhances the difference in Δ further.

Both the ligands pyridine and bipyridyl have π-orbitals. For complexes with transition metals it is generally found the involvement of the empty anti-bonding π-orbitals to be predominant over that of the filled bonding π-orbitals, so that π-bonding in this case stabilizes the d_{xy}, d_{yz} and d_{xz} orbitals of the metal ion. However, since the complexes studied here contain tetravalent central ions it is very unlikely that the π-accepting effect by pyridine and bipyridyl is very important. Even so it seems reasonable to

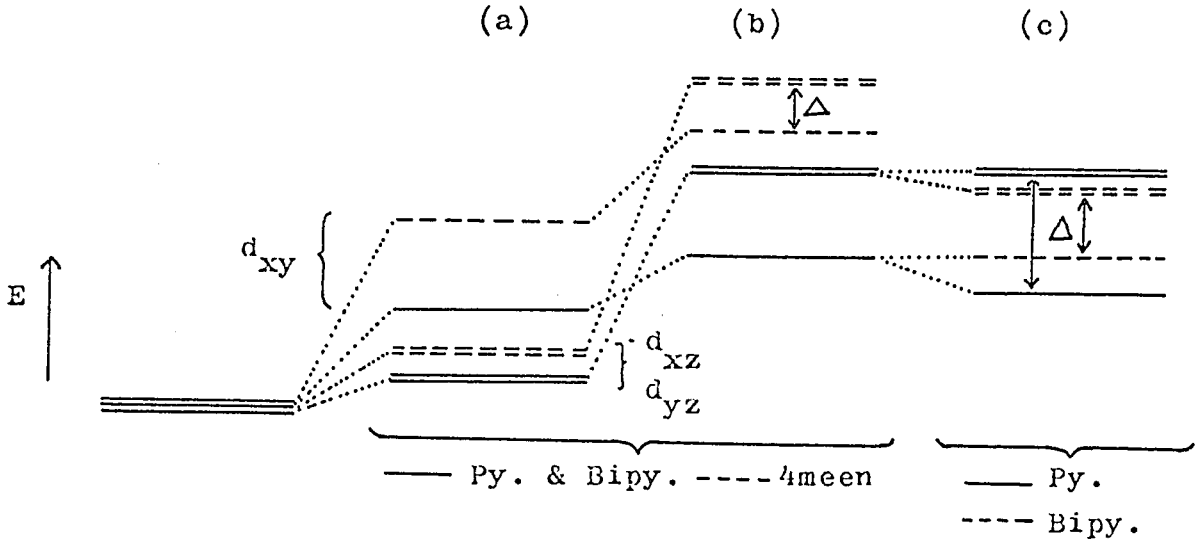

Figure 21. Schematic diagram of the effects of various metal-ligand interactions on d_{xz}, d_{yz} and d_{xy}.
(a) Electrostatic, (b) π-donor from halogens along z-axis, and (c) π-acceptor effect by py. and bipy.

attribute the difference in the values of Δ (and therefore μ_{eff}) between the complexes of NbX_4 with pyridine and 2,2'-bipyridyl to the difference in the degree with which the two can act as π-acceptors. Referring to the figure of the di-substituted cis-complex (page 65), it is seen that whereas the bipyridyl cannot form a π-bond with the d_{xy} orbital, the pyridine rings, since they are most probably not coplanar, can probably do so. Similarly, pyridine probably does not form as strong a π-bond as bipyridyl with d_{xz} and d_{yz}. The net result is that the separation of d_{xy} from d_{xz} and d_{yz}, i.e. Δ, is larger for the pyridine complex. This is shown in figure (21). Thus Δ decreases in the order pyridine > bipyridyl > tetramethylethylenediamine.

APPENDIX I

Transformation Properties of d-orbitals in D_{4h}

	E	C_4	C_2	C_2'	C_2''
d_2	d_2	$-d_2$	d_2	d_{-2}	$-d_{-2}$
d_1	d_1	$-id_1$	$-d_1$	d_{-1}	$-id_{-1}$
d_0	d_0	d_0	d_0	d_0	d_0
d_{-1}	d_{-1}	id_{-1}	$-d_{-1}$	d_1	$-id_1$
d_{-2}	d_{-2}	$-d_{-2}$	d_{-2}	d_2	$-d_2$
χ	5	-1	1	1	1

REFERENCES

1. P.W. Selwood, "Magnetochemistry," 2nd Ed. Interscience, New York (1956).
2. R.S. Nyholm, Quart. Rev., 7, 377 (1953).
3. B.N. Figgis and J. Lewis, in "Modern Coordination Chemistry," J. Lewis and R.G. Wilkins (Editors), Interscience,New York (1960).
4. R.S. Nyholm, J. Inorg. Nucl. Chem., 8, 401 (1958).
5. J.H. Van Vleck, "Electronic and Magnetic Susceptibilities," Oxford Univ. Press, Oxford and New York (1932).
6. C.J. Ballhausen, "Introduction to Ligand Field Theory," McGraw-Hill,New York (1962).
7. H. Bethe, Ann. Phys., 3, 133 (1929).
8. R. Schlapp and W.G. Penney, Phys. Rev., 42, 666 (1932).
9. B.N. Figgis, J. Inorg. Nucl. Chem., 8, 476 (1958).
10. B. Bleaney and K.W. Stevens, Report Prog. Phys., 16, 108 (1953).
11. J.B. Howard, J. Chem. Phys., 3, 813 (1935).
12. J. Owen, Proc. Roy. Soc. (London), A227, 183 (1955).
13. M. Kotani, J. Phys. Soc. Japan, 4, 293 (1949).
14. B.N. Figgis, Nature, 182, 1568 (1958).
15. W. Moffitt, G.L. Goodman, M. Fred and B. Weinstock, Mol. Phys., 2, 109 (1959).
16. H. Kamimura, S. Koide, H. Sekiyama and S. Sugano, J. Phys. Soc. Japan, 15, 1264 (1960).
17. H.A. Jahn and E. Teller, Proc Roy. Soc. (London), A161, 220 (1937).
18. B.N. Figgis, J. Chem. Soc., 1965, 4887.
19. F.A. Cotton, "Chemical Applications of Group Theory," Interscience,New York (1963).

20. B.N. Figgis and J. Lewis, in "Progress in Inorganic Chemistry, " F.A. Cotton (Editor), Vol. 6, 37 (1964).

21. M. Tinkham, Proc.Roy. Soc. (London), A236, 535 and 549 (1956).

22. J.H.E. Griffiths, J. Owen, I.M. Ward, Proc. Roy. Soc. (London), A219, 526 (1953).

23. B. Bleaney and M.C.M. O'Brien, Proc. Phys. Soc. B69, 1216 (1956).

24. K.W.H. Stevens, Proc. Roy. Soc. (London), A219, 542 (1953).

25. C.J. Ballhausen, in "Advances in the Chemistry of Coordination Compounds," S. Kirschner (Editor), Macmillan Co.New York (1961), page 3.

26. F.A. Cotton, J. Chem. Educ. 41, 466 (1964).

27. R.S. Mulliken, Phys. Rev., 40, 55 (1932).

28. H.B. Gray, J, Chem. Educ. 41, 2 (1964).

29. C.J. Ballhausen and H.B. Gray, "Molecular Orbital Theory," Benjamin Inc.New York (1964), chapter 8.

30. S.F.A. Kettle, J. Chem. Educ. 43, 21 (1966).

31. L.E. Orgel, "Transition-Metal Chemistry," Methuen Co. Ltd. London (1960).

32. H. Kamimura, J. Phys. Soc. Japan, 11, 1171 (1956).

33. J.S. Griffith, "The Theory of Transition-Metal Ions," Cambridge Univ. Press, Cambridge (1961).

34. B.N. Figgis,Trans. Faraday Soc., 57, 198 (1961).

35. B.N. Figgis, Trans. Faraday Soc., 57, 204 (1961).

36. P.C.H. Mitchell, R.J.P. Williams, J. Chem. Soc., 1962, 4571.

37. G.W.A. Fowles and R.A. Hoodless, J. Chem. Soc., 1963, 33.

38. M.W. Duckworth, G.W.A. Fowles and R.A. Hoodless, J. Chem. Soc., 1963, 5665.

39. M. Schläfer and R. Götz, Z. Anorg. Allgem. Chem., 328, 1 (1964).

40. R.J.H. Clark, J. Lewis, D.J. Machin and R.S. Nyholm, J. Chem. Soc., 1963, 379.

41. R.J.H. Clark, J. Chem. Soc., 1965, 5699.

42. R.J.H. Clark, J. Chem. Soc., 1963, 1377.

43. D. Brown, J. Chem. Soc., 1964, 4944.

44. R.E. McCarley and B.A. Torp, Inorg. Chem., 2, 540 (1963).

45. R.E. McCarley and J.C. Boatman, Inorg. Chem. 2, 547 (1963).

46. M. Allbutt, K. Feenan and G.W. Fowles, J. Less-Common Metals, 6, 299 (1964).

47. G.B. Hargreaves and R.D. Peacock, J. Chem. Soc., 1958, 3776.

48. J.H. Garside, J. Chem. Soc., 1965, 6634.

49. E.A. Allen, B.J. Brisdon, D.A. Edwards, G.W.A. Fowles and R.G. Williams, J. Chem. Soc., 1963, 4649.

50. K.W. Bagnall, D. Brown and J.G.H. Du Preez, J. Chem. Soc., 1964, 2603.

51. R.N. Dickinson, S.E. Feil, F.N. Collier, W.W. Horner, S.M. Horner and S.Y. Tyree, Inorg. Chem., 3, 1600 (1964).

52. B.J. Brisdon and R.A. Walton, J. Chem. Soc., 1965, 2274.

53. D. Brown and R. Colton, J. Chem. Soc., 1964, 714.

54. K.W. Bagnall, D. Brown and R. Colton, J. Chem. Soc., 1964, 3017.

55. H.R. Nettleton and S. Sugden, Proc. Roy. Soc. (London), A173, 313 (1959).

56. L.F. Bates, "Modern Magnetism," 4th Ed. Cambridge Univ. Press, Cambridge (1961), page 115.

57. B.N. Figgis and R.S. Nyholm, J. Chem. Soc., 1958, 4190.

58. B.N. Figgis and R.S. Nyholm, J. Chem. Soc., 1959, 338.

59. H. Shäfer and F. Kahlenberg, Z. Anorg. Allgem. Chem., 305, 178 (1960).

60. G. Fritz, D. Havel, D. Kummer and G. Teichman, Z. Anorg. Allgem. Chem., 302, 60 (1959).

61. International Critical Tables, McGraw-Hill, New York (1929), VI, 361.

62. I.R. Beattie and M. Webster, J. Chem. Soc., 1964, 3507.

63. B.A. Torp, Ph.D. Thesis, Iowa State University (1964), Diss. Abst., 25, 2751 (1964).

64. D.S. McClure, in "Advances in the Chemistry of Coordination Compounds," S. Kirschner (Editor), Macmillan Co. New York (1961), page 498.

65. J.S. Griffith and L.E. Orgel, J. Chem. Soc., 1956, 4981.